Hydrogen Plasma Processing of Iron Ore

KALI CHARAN SABAT and ANTHONY B. MURPHY

Iron is currently produced by carbothermic reduction of oxide ores. This is a multiple-stage process that requires large-scale equipment and high capital investment, and produces large amounts of CO_2. An alternative to carbothermic reduction is reduction using a hydrogen plasma, which comprises vibrationally excited molecular, atomic, and ionic states of hydrogen, all of which can reduce iron oxides, even at low temperatures. Besides the thermodynamic and kinetic advantages of a hydrogen plasma, the byproduct of the reaction is water, which does not pose any environmental problems. A review of the theory and practice of iron ore reduction using a hydrogen plasma is presented. The thermodynamic and kinetic aspects are considered, with molecular, atomic and ionic hydrogen considered separately. The importance of vibrationally excited hydrogen molecules in overcoming the activation energy barriers, and in transferring energy to the iron oxide, is emphasized. Both thermal and nonthermal plasmas are considered. The thermophysical properties of hydrogen and argon–hydrogen plasmas are discussed, and their influence on the constriction and flow in the of arc plasmas is considered. The published R&D on hydrogen plasma reduction of iron oxide is reviewed, with both the reduction of molten iron ore and in-flight reduction of iron ore particles being considered. Finally, the technical and economic feasibility of the process are discussed. It is shown that hydrogen plasma processing requires less energy than carbothermic reduction, mainly because pelletization, sintering, and cokemaking are not required. Moreover, the formation of the greenhouse gas CO_2 as a byproduct is avoided. In-flight reduction has the potential for a throughput at least equivalent to the blast furnace process. It is concluded that hydrogen plasma reduction of iron ore is a potentially attractive alternative to standard methods.

DOI: 10.1007/s11663-017-0957-1

I. INTRODUCTION

Almost all economically important metals are extracted from naturally occurring ores. Of these metals, the d-block transition metals play a particularly significant role in our day-to-day life. These transition metals have assumed utmost importance due to our ever-growing population and economy. The most widely used transition metal in modern times is iron, in the form of steel. Globally, iron and steel production has surpassed 1660 million tonnes per annum, and is increasing day-by-day.[1]

Steel production is not only energy intensive, but also environmentally sensitive, at a time when climate change is a great concern throughout the world. The steel industry has been successful in reducing the energy consumption per tonne of steel by 60 pct in the last 50 years. This drastic change leaves little room for improvement of conventional technologies. Of these technologies, blast furnace–basic oxygen furnace—accounts for 70 pct of the total world steel production.[2]

The blast furnace–basic oxygen furnace process requires huge capital investments and is highly energy intensive. The feedstock used by the process includes sinters or pellets from medium/high-grade iron ore and coke, manufactured from coking coal. Both medium/high-grade iron ore and coking coal are being depleted, placing limitations on future supply. Pelletization, sintering, and cokemaking, are problematic and costly steps, and are also facing tighter regulation. The process requires the use of carbon, leading to the emission of the greenhouse gas CO_2 into the atmosphere; for every tonne of steel produced, 1.8 tonnes of CO_2 is emitted. As a consequence, the iron and steel industry is responsible for 6.7 pct of total global CO_2 emissions.[2] Climate change associated with the emission of CO_2 and other greenhouse gases is pushing the world into a dangerous realm, with consequences including shrinking glaciers, rising sea levels, heat waves, destruction of ecosystems, loss of biodiversity, and economic losses.[3] There have been considerable efforts worldwide to decrease CO_2 emissions from the steel industry; however, the blast furnace—basic oxygen furnace process is a mature technology, and advanced facilities operate close to thermodynamic equilibrium. Therefore, a significant reduction of CO_2 emissions using conventional technologies does not seem feasible.[4]

Although a number of myths have been propagated about the steel industry, such as 'the steel industry is mature,' and the steel industry is dying,' there is in fact a

KALI CHARAN SABAT is with the Project & Environment Cell, Visiontek Consultancy Services Pvt. Ltd., Bhubaneswar, Odisha, 751016, India and also with the School of Mechanical Engineering, KIIT University, Bhubaneswar, Odisha, 751016, India. Contact e-mails: kcsabat@gmail.com, kcsabat@vcspl.org ANTHONY B. MURPHY is with the CSIRO Manufacturing, PO Box 218, Lindfield, NSW, 2070, Australia.

Manuscript submitted November 12, 2015.
Article published online March 16, 2017.

rapid growth in demand for iron and steel.[5] In order to keep pace with this demand, and as a response to the problems faced by the blast-furnace—basic-oxygen-furnace process, considerable research has been and continues to be performed on low-carbon breakthrough technologies worldwide, including in the EU (ULCOS), Japan (COURSE50), US (AISI), Canada (The Canadian Steel Producers Association), South Korea (POSCO), China (Bao Steel & China Steel) and Australia (CSIRO, Bluescope Steel and One Steel). To date, about US $1 billion has been invested in these R&D projects, the highest investments being in the ULCOS I (US $95 million) and ULCOS II (US $630 million) technologies.[2] These programs have identified the steelmaking technologies with the most promise of reducing CO_2 emissions by more than 50 pct. Hydrogen stands out as the strongest candidate for an alternative reductant in place of carbon (ULCOS II, COURSE50, POSCO, *etc.*).[6–10]

Hydrogen shows several technical advantages: (a) the product gases are mixtures of H_2O and H_2, thereby avoiding CO and CO_2, (b) thermodynamic and kinetic considerations mean that the reduction rate is fast,[10–15] (c) its use avoids carbon content in the produced iron, and (d) it allows the use of metallurgical coke, which is polluting and expensive, to be avoided. The consumption of hydrogen is much low than that of carbon, as shown in Table I.[11] Further, it has been recently reported that energy consumption is reduced by 32 or 57 pct, and CO_2 emissions are reduced by 61 or 96 pct, compared with blast furnace ironmaking, for natural gas and hydrogen, respectively, as the reductant/fuel.[15] These benefits come mainly due to the elimination of coke making and sintering or pelletization.[15] For a detailed and comprehensive discussion on ironmaking, the reader is referred to References 16 through 18.

Some ambitious projects are underway using hydrogen as an alternative reductant.[19,20] The objective is to produce liquid steel directly from iron ore, and hence these processes are called direct steelmaking processes.[21] They can be divided into two groups: shaft-furnace and fluidized-bed processes.

The shaft-furnace processes are direct reduction processes that utilize the higher reactivity of hydrogen, relative to carbon monoxide, for reduction of iron ore at lower operating temperatures. The dominant shaft-furnace processes are MIDREX[22] and HYL.[23–25] However, the shaft furnaces require a pelletization step, which entails additional cost and environmental problems. Further, shaft furnaces cannot match the large production rates of blast furnaces, due to the problems with the sticking and fusion of particles[26,27] and pellet disintegration.[28–31]

The fluidized-bed processes are direct reduction or smelting processes that use iron ore fines. Iron ore fines, in this context, correspond to the majority of individual particles measuring less than 10 mm diameter. POSCO's FINEX,[32–37] Lurgi's CICRORED,[38–40] and the FIOR,[41] FINMET,[33–42] and Iron Carbide[43] processes are the representative large-scale applications of the technology.

It has been recently reported that the low-grade fine iron ore concentrates, in this case particles of size less than 100 μm, can be reduced with hydrogen gas in small-scale units, bypassing problematic and costly steps such as pelletization, cokemaking, and sintering.[44] In this context, a new technology using hydrogen gas, named 'suspension ironmaking technology' is under development at the University of Utah.[19,20] The process is essentially the first flash-type ironmaking process, in which the fine iron ore concentrate is converted directly to metallic iron by in-flight reduction with molecular hydrogen. The use of dilute particle suspension greatly diminishes sticking and fusion problems, so the proposed process can be operated at high temperatures, allowing high intensities, and ensuring favorable thermodynamics. The raw materials can be fed easily, and it is possible to produce either solid or molten iron. The material and energy balance calculation of their process shows that the process reduces energy consumption, compared with the blast furnace, by 38 pct and CO_2 emission by 96 pct.[19] The process should be readily adaptable to a large-scale reactor.

There have also been studies performed of an in-flight reduction process using heated but nonionized hydrogen gas. Since the process is easily adaptable to HP, we consider it later in this paper (in Section VI–B–2) in the context of related HP processes.

Hydrogen in the plasma state provides thermodynamic and kinetic advantages for reduction because of the presence of atomic, and ionic, as well as vibrationally excited, hydrogen species. The energy carried by these species can be released at the reduction interface, leading to local heating. Thus, reduction by hydrogen plasma (HP) does not require volumetric heating, as is required for molecular hydrogen. This allows the heat loss from the reactor to be reduced, with accompanying cost savings. It has been reported that steel of high quality and productivity can be produced using a HP, with a cost saving of 20 pct compared with the blast furnace process.[45]

Although hydrogen is the preferred reductant fuel from the environmental and reduction kinetics viewpoints, it is currently expensive.[46] Nevertheless, there are widespread expectations for the development of the hydrogen economy, and thus the availability of

Table I. Masses of Reductants and Products in Case of Reduction of Hematite to Iron

Reaction	C	CO	CO_2	H_2	H_2O
$Fe_2O_3 + 3C \rightarrow 2Fe + 3CO$	36	84			
$Fe_2O_3 + 3/2C \rightarrow 2Fe + 3/2CO_2$	18		66		
$Fe_2O_3 + 3H_2 \rightarrow 2Fe + 3H_2O$				6	54

Tonnes per 112 tonne of Fe

inexpensive hydrogen; much effort and many resources are being devoted toward this goal.[46] Production of hydrogen currently uses either reforming of methane or electrolysis of water, both of which are energy intensive processes. However, there is a large research effort devoted to using solar energy for the production of hydrogen, for example through use of solar cells to provide the electrons necessary to electrolyse water, or through photocatalytic water splitting, in which the action of sunlight on a semiconductor immersed in water is used to produce hydrogen directly.[47,48]

HP reduction of iron oxide can occur for different physical states of iron oxide. Depending on the physical state of the reacting iron oxide at the reaction interface, we divide the HP reduction of iron oxide into two classes: heterogeneous processes, in which the reduction reactions occur at the interface between the HP and the molten or solid iron oxide, and homogeneous processes, in which the iron oxide is vaporized, so reactions occur in the gas phase. Homogeneous processes can also be referred to as dissociative reduction.[11] The great majority of processes investigated are heterogeneous, but we consider homogeneous processes as well, both for completeness and because their characteristics are instructive.

This review builds on earlier publications,[11–14] which provided a general overview of the reduction of metal oxides by HPs,[11] study of HP reduction of cobalt oxide[12] and copper oxide,[49] and experimental studies of the reduction of iron oxide in a microwave HP.[13,14] We refer on several occasions to[11] in particular, to avoid unnecessary duplication.

Our review is structured as follows. We begin in Section II with a brief introduction to plasmas of industrial interest, emphasizing the difference between thermal and nonthermal plasmas. We then discuss the thermodynamics of the hydrogen reduction process in Section III, with particular emphasis on the advantages associated with vibrationally excited hydrogen molecules and atomic hydrogen, which are produced in plasma processes. We also consider the relevance of hydrogen ions, taking into account the influence of charging of the melt.

The reduction of iron oxide by thermal HP involves three steps: (i) transfer of HP species from the gas or plasma to the HP–iron-ore reduction interface, (ii) reduction reactions at the interface, and (iii) transfer of the products from the interface to the bulk of the respective phases. Of these, the second step is controlled by thermodynamics and reaction kinetics; at the high temperatures of thermal HP, these factors are generally favorable. The overall reduction kinetics is then controlled by the first and third steps, which depends on the transfer of heat, mass, and momentum. Therefore, we examine in Section IV the thermophysical properties of hydrogen and argon–hydrogen thermal plasmas.

This is followed in Section V by an examination of the kinetics of the hydrogen reduction process, as well as departures from equilibrium of atomic hydrogen generation, as occur in nonthermal plasmas, and in some regions of thermal plasmas.

We then, in Section VI, review the published experimental studies on reduction of iron ore by HP. We first consider the relatively few experimental studies of reduction of iron oxide in nonthermal HP. This is followed by a detailed review of the published work on reduction of iron ore by thermal HPs. Processes in which the HP reduces liquid iron oxide at the interface between the plasma and the ore, and in-flight reduction processes, are both considered.

Finally, in Section VII, we consider the technical and economic feasibility of HP reduction of iron ore, looking in particular at the energy efficiency and throughput compared with conventional processes.

II. FUNDAMENTALS OF PLASMAS

Plasmas are known as the fourth state of matter. A plasma is formed when sufficient energy is transferred to a gas to partially ionize the molecules or atoms. The vast majority of the universe including stars and the interstellar medium, is in the plasma state. On Earth, plasmas occur in lightning and in flames, and are applied in many industrial processes.

Plasmas of industrial interest can be divided into two main classes: thermal and nonthermal plasmas. (Here we do not consider plasmas used in experimental devices aimed at producing nuclear fusion, which is not yet an industrial process.)

A. *Thermal Plasmas*

Thermal plasmas are at pressures above about 0.1 atm. They can be produced between two electrodes by a DC or AC voltage, or by a radiofrequency or microwave electromagnetic field. Initially the electrons are heated, but the high pressure ensures a high rate of collisions between the electrons and heavy species (molecules, atoms, and ions), so that the temperatures of the electrons and heavy species rapidly reach equilibrium. This gives rise to the property of local thermodynamic equilibrium (LTE), which requires that all the temperatures (translational temperatures of electrons and heavy species, electronic, vibrational, and rotational excitation temperatures of atoms and molecules, and the equilibrium temperature of chemical reactions) are equal at a given position.

LTE is usually a valid assumption in the central regions of thermal plasmas produced by a DC or AC voltage, or by a radiofrequency electromagnetic field. Deviations can occur near electrodes, and in the fringes of the plasma, with electron temperatures being higher than the heavy-species temperature in these regions. Examples relevant to HPs will be considered in Section V–B. Microwave plasmas usually have strong deviations from LTE, with the electron temperature 2 to 10 times higher than the heavy-species temperature.

Typical thermal plasma temperatures are in the range of 5000 K to 25,000 K (4727 °C to 24,727 °C), and typical electron densities are of the order of 10^{23} m^{-3} in the case of atmospheric pressure, corresponding to complete first ionization of all atoms. Figure 1 shows the calculated composition of an LTE HP at 1 atm for temperatures up to 30,000 K (29727 °C). The hydrogen

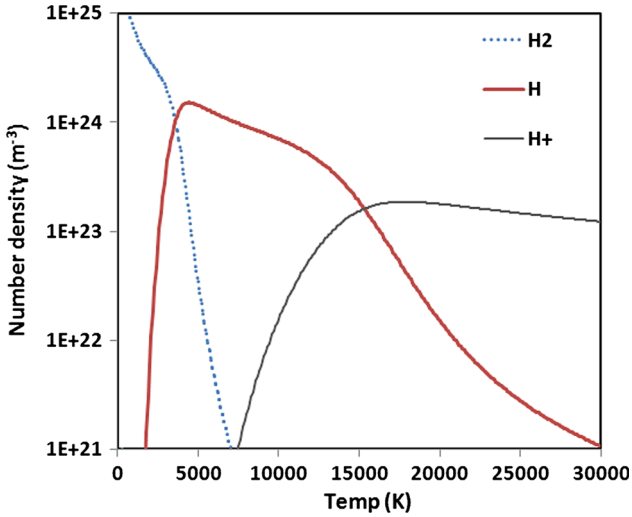

Fig. 1—The temperature dependence of species number densities in a hydrogen plasma in local thermodynamic equilibrium at 1 atm.[62–64]

is 50 pct dissociated at about 3500 K (3227 °C), and 50 pct ionized at about 15,000 K (14,727 °C).

As energy is added to the hydrogen molecule, it moves from the ground state to higher rotational and then vibrational levels. These levels have relatively long lifetimes. The first rotational level is only 0.015 eV above the ground state, and the first vibrational level is 0.516 eV above the ground state.[50] The energies required to access these excited states are much less than the 5.42 eV required for dissociation. Dissociation typically occurs stepwise, as a molecule gains energy through collisions and moves into increasingly high rotational and vibrational levels. As hydrogen gas is heated, the proportion of molecules in a given rovibrational level increases according to the Boltzmann distribution. More detail is given in Section V–C.

DC thermal plasmas can be divided into transferred arcs (in which one of the electrodes is the work piece, *i.e.*, the charge or melt in metallurgical applications) and nontransferred arcs, in which the arc is between two electrodes within a plasma torch, and a jet of plasma issuing from the torch is used for the process.

Applications of thermal plasmas include arc welding, plasma spraying, plasma cutting, arc furnaces, and other metallurgical applications, arc lighting, waste treatment, nanoparticle production, and particle spheroidization. These applications make use of the high temperatures, high heat fluxes, and strong radiative emission, which characterize thermal plasmas.

B. *Nonthermal Plasmas*

Nonthermal plasmas are also known as nonequilibrium or cold plasmas. In such plasmas, the electron temperature is very much higher than the heavy-species temperature. As in thermal plasmas, the electrons are initially heated by an electric or electromagnetic field. However, in nonthermal plasmas, the electrons do not efficiently transfer energy to the heavy species. This can be due to operation at a low pressure, with a consequent reduction in collision rate. Nonthermal plasmas can also be produced at atmospheric pressure by ensuring the lifetime of the plasma is very short (well below a microsecond); in this case there is insufficient time for the electrons to heat the heavy species. This can be achieved by inserting a dielectric barrier between the two electrodes to which an AC voltage is applied; the build-up of charge on the dielectric interrupts the discharge, which resumes when the polarity is reversed.

Nonthermal plasmas are characterized by several temperatures, including the translational or kinetic temperatures of electrons (T_e), ions (T_i) and neutrals (T_g), and the vibrational (T_v) and rotational (T_r) excitation temperatures of molecules. These are generally referred to as the electron, ion, gas, vibrational, and rotational temperatures, respectively. Typically they follow the order $T_e > T_v > T_r \approx T_i \approx T_g$.[51,52] In many nonthermal plasma systems, T_e is about 1 eV (~11,600 K (11,327 °C)), while T_g is close to room temperature.

Low-pressure plasmas are used for applications including etching of semiconductors and thin-film deposition. Applications of atmospheric-pressure nonthermal plasmas include ozone production, gas cleaning, modifying the surface properties of plastics, and plasma displays.

III. THERMODYNAMICS OF THE REDUCTION PROCESS

Thermodynamic and kinetic principles provide guidance toward potential pathways for the reduction of metal oxides. The spontaneity or feasibility of the reduction is established by its Gibbs standard free energy change ($\Delta G°$). For a reduction to be spontaneous, $\Delta G°$ should be negative. The Ellingham diagram provides $\Delta G°$ of oxides as a function of temperature (T).[11,45] The diagram gives an estimate of how changes in T, pressure (P) and composition affect the chemical equilibrium of oxides, thereby providing information as to the stability as well as the possibility of reduction of oxides. An Ellingham diagram for a wide range of metal oxides is given in Figure 2.

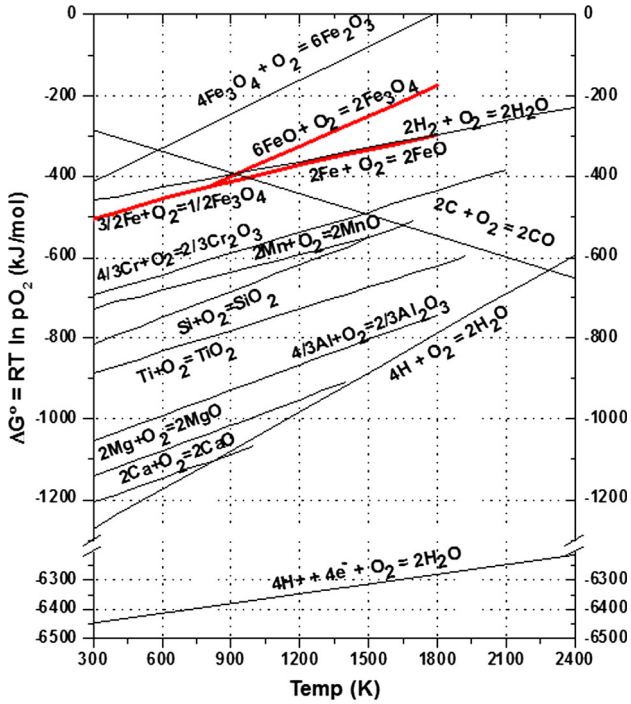

Fig. 2—Ellingham diagram for metal-oxide conversion, showing MO-M, H_2O-H_2, H_2O-H, and H_2O-H^+ lines.

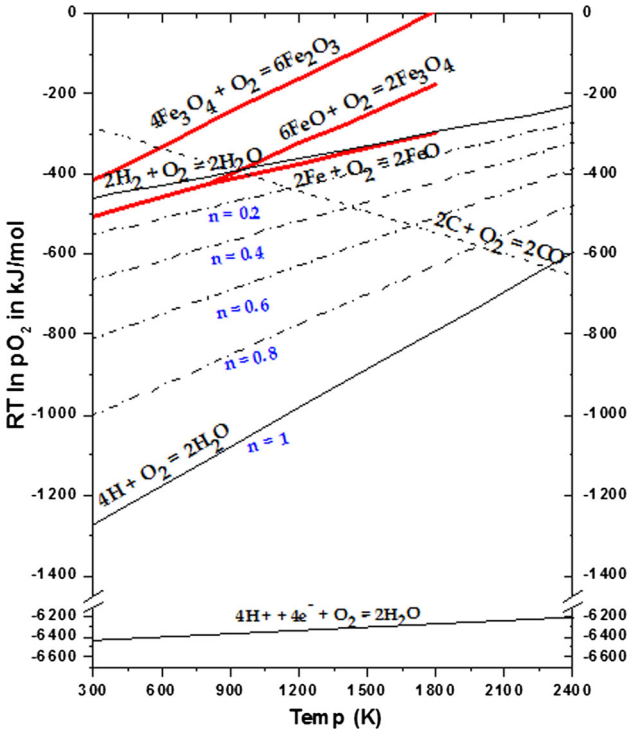

Fig. 3—The Ellingham diagram of iron oxides, including hydrogen species, showing the influence of different levels n of dissociation of H_2.

The Ellingham diagram of iron oxides, including hydrogen species, is presented in Figure 3. An elemental reactant associated with a given line can reduce an oxide associated with a line at larger ΔG°.

As evident from Figure 3, the H_2–H_2O line lies below the lines of hematite (Fe_2O_3) and, for temperatures above 900 K (627 °C), magnetite (Fe_3O_4). H_2 should therefore reduce these iron oxides. In practice, this does not happen, due to thermodynamic and kinetic constraints. Now, some kinetic features of gaseous reduction of iron ore are well established.[53–60] The reduction of iron ore by H_2 occurs in stages, $Fe_2O_3 \rightarrow Fe_3O_4 \rightarrow Fe_xO \rightarrow Fe$. Fe_xO, whose mineralogical name is wustite, has significant stoichiometric variability, with x assuming values from 0.83 to 0.955. Assuming $x = 1$ for simplicity, the fractional oxygen removals are 1/9, 2/9, and 6/9, respectively. The corresponding reduction reactions can be presented by the reactions:

$$3Fe_2O_3 + H_2 = 2Fe_3O_4 + H_2O \qquad \Delta G_1^\circ = 3.0 - 0.1096T\,(T \text{ in K}) \qquad [1]$$

$$Fe_3O_4 + H_2 = 3FeO + H_2O \qquad \Delta G_2^\circ = 65.75 - 0.702T\,(T \text{ in K}) \qquad [2]$$

$$FeO + H_2 = Fe + H_2O \qquad \Delta G_3^\circ = 18.45 - 0.102T\,(T \text{ in K}) \qquad [3]$$

the overall reaction being

$$Fe_2O_3 + 3H_2 = 2Fe + 3H_2O \qquad \Delta G_4^\circ = 37.57 - 0.0432T\,(T \text{ in K}) \qquad [4]$$

As seen from the ΔG° in the above equations, the thermodynamically favorable steps in iron oxide reduction are $Fe_2O_3 \rightarrow Fe_3O_4$ and $Fe_3O_4 \rightarrow FeO$, at temperatures above 900 K (627 °C). So these steps can be carried out by removing the kinetic barrier. The final step, $FeO \rightarrow Fe$, which entails the greatest fractional oxygen removal (6/9), is not only endothermic but also ΔG° positive. For example, at 1673 K (1400 °C), ΔG_3° = 3.76 kJ/mol.[61] The hydrogen reduction of $Fe_2O_3 \rightarrow FeO$ has a large equilibrium constant, *i.e.*, it is essentially irreversible, while in contrast $FeO \rightarrow Fe$ has an equilibrium constant that strongly favors the reverse reaction.[61] This is indicated by the location of the H_2–H_2O line above the Fe–FeO line in Figure 3. In order to move the H_2–H_2O line downward to a position below Fe–FeO line, to make $FeO \rightarrow Fe$ feasible, the use of a HP becomes important.

When the H_2 is provided with sufficient energy ($h\nu$), it converts to a HP containing rotationally and vibrationally excited (or using more concise terminology, rovibrationally excited), hydrogen molecules (H_2^*), monoatomic hydrogen (H), and ionic hydrogen (H^+.). The energy can be either supplied by thermal heating or electric discharges (DC, microwave, radio-frequency, inductively coupled, *etc.*).

The HP can be represented by

$$H_2(g) + h\nu = HP\left(H_2^*/2H/2H^+\right) \quad \Delta G_5^\circ \gg 0 \qquad [5]$$

The distribution of different excited species in a HP in local thermodynamic equilibrium at atmospheric pressure was given in Figure 1.[62–64]

The overall reaction for reduction of FeO by an HP can be obtained by thermodynamic coupling of Eqs. [3] through [5]. This leads to

$$\mathrm{FeO} + \mathrm{HP}\left(\mathrm{H}_2^*/2\mathrm{H}/2\mathrm{H}^+\right) = \mathrm{Fe} + \mathrm{H_2O}$$

$$\Delta G_6^\circ = \Delta G_3^\circ - \Delta G_5^\circ < 0 \qquad [6]$$

The ΔG° becomes negative (indicating that reduction is feasible) even at low T. Here, T refers to the temperature of all the species present at the reduction interface under local thermodynamic equilibrium in a thermal plasma. It should be noted that the effect of H_2^* on ΔG° has not yet been reported. The stored energy in H_2^* will, however, increase the rate of dissociation,[65] as will be discussed in Section V–C. However, the H and H^+ present in the plasma decrease ΔG° by around 900 and 6000 kJ/mol, respectively,[11] as shown in Figure 3. This decrease in ΔG° indicates the importance of the HP in the reduction of iron oxides.

A. *Role of Monatomic Hydrogen*

Hydrogen removes the oxygen from iron oxide by oxidation. The ΔG° values for oxidation of H_2 and H are given by References 66 and 67:

$$2\mathrm{H_2} + \mathrm{O_2} = 2\mathrm{H_2O} \quad \Delta G_7^\circ = -492.9 + 0.1096T\,(T \text{ in K}) \qquad [7]$$

$$4\mathrm{H} = 2\mathrm{H_2} \quad \Delta G_8^\circ = -875.61 + 0.21205T\,(T \text{ in K}) \qquad [8]$$

$$4\mathrm{H} + \mathrm{O_2} = 2\mathrm{H_2O} \quad \Delta G_9^\circ = -1368.51 + 0.3267T\,(T \text{ in K}) \qquad [9]$$

ΔG° is dependent on the physically measurable quantities of equilibrium partial pressure (p) and T. The p of H_2 or H required for the reduction of different iron oxides with hydrogen is determined from the equilibrium constant, which is in turn determined from ΔG°. The temperature dependence of the partial pressure of H_2 and H required for the reduction of iron oxides is shown in Figures 4(a) and (b), respectively; the diagrams have been drawn from the data taken from the literature.[66–69] As shown in Figure 4(a), the reaction $Fe_2O_3 \rightarrow Fe_3O_4$ is thermodynamically feasible at all temperatures at very low p of H_2 (~10^{-4} to 10^{-5}). The other two reduction steps ($Fe_3O_4 \rightarrow FeO$ and $FeO \rightarrow Fe$) require higher p. But unlike H_2, the p required for H for these reactions is very low, as shown in Figure 4(b).

Such low partial pressures of H can be obtained using a nonthermal plasma, favoring the production of iron by direct reduction of iron oxides.[11–14] Although the required p of H is low, H is unstable with a short lifetime (~4 ms), while H_2 is of course stable,[8] and a pure H atmosphere cannot be created. However, mixtures of H and H_2 with varying fractions of H can be produced. These metastable mixtures have usable lifetimes.[70] These mixtures may be applicable to reduction of iron oxides. Deviations from chemical equilibrium can produce enhanced concentrations of H in thermal plasmas as well, as will be discussed in Section V–B.

The H and H_2 equilibria are described in Eqs. [7] through [9]. Assuming that the hydrogen gas mixture consists of only H and H_2, and the mixture obeys the ideal gas law *i.e.*, $\frac{p_H}{p_{H_2}} = \frac{n_H}{n_{H_2}}$, where p and n represent the partial pressure and the number of moles of the components, respectively, the mixture of H and H_2 reacts with the oxygen in FeO to form water vapor according to the following stoichiometry:

$$n_H\mathrm{H} + n_{H_2}\mathrm{H_2} + \left(\frac{n_H}{4} + \frac{n_{H_2}}{2}\right)\mathrm{O_2} = \left(\frac{n_H}{2} + n_{H_2}\right)\mathrm{H_2O} \qquad [10]$$

As discussed in Reference 11 ΔG_{10}° for this reaction is calculated from $\Delta G_7^\circ$and ΔG_9° as

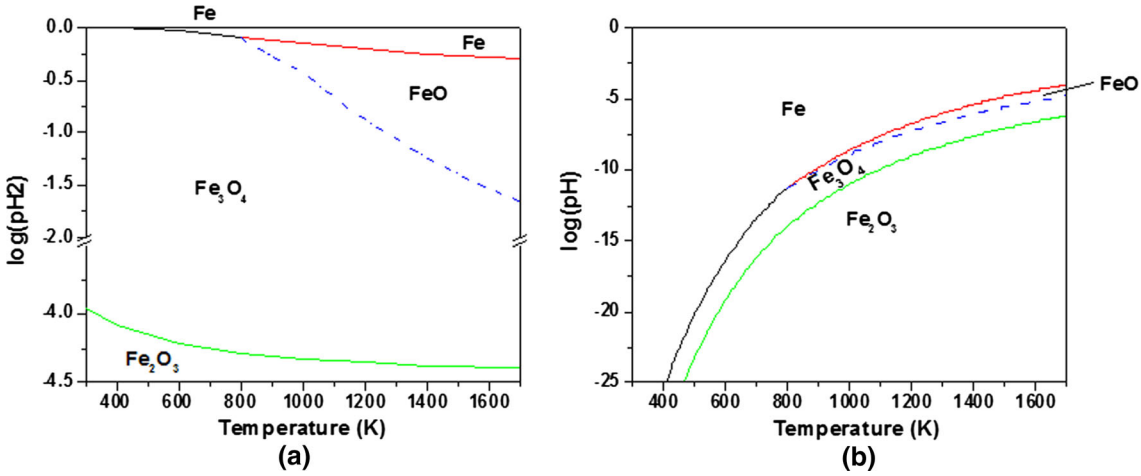

Fig. 4—Equilibrium partial pressures for reduction by (*a*) molecular hydrogen and (*b*) atomic hydrogen.

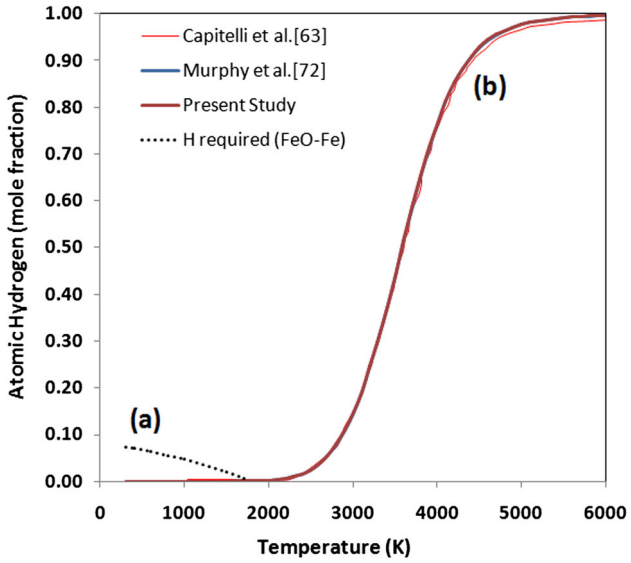

Fig. 5—Dependence of mole fraction of atomic hydrogen on temperature at atmospheric pressure: (*a*) H required for reduction of FeO; and (*b*) H obtainable under LTE conditions; the results of Murphy *et al.*[63] and Capitelli *et al.*[72] are shown for comparison.

$$\Delta G^{\circ}_{10} = \frac{1}{2-n}\left[-985.75 - 382.75n + (0.21924 + 0.10242n)\,T\right] \quad [11]$$

where n is the mole fraction of atomic hydrogen. It was shown in Reference 11 that ΔG_{10}° decreases as n increases.

The value of ΔG° for $2Fe + O_2 = 2FeO$ is given by Reference 66

$$\Delta G^{\circ}_{11} = -529.8 + 0.1307T (T \text{ in K}) \quad [12]$$

The reduction of FeO by a mixture of H and H_2 can be represented by

$$\frac{4n}{2-n}H + \frac{4(1-n)}{2-n}H_2 + 2FeO = 2H_2O + 2Fe \quad [13]$$

The ΔG° for this reduction reaction is $\Delta G^{\circ}_{12} = \Delta G^{\circ}_{10} - \Delta G^{\circ}_{11}$.

Using the values of ΔG°_{10} and ΔG°_{11}, at equilibrium (*i.e.* $\Delta G^{\circ}_{12} = 0$), the mole fraction of H required for reduction of FeO as a function of T is given by

$$n = (73.85 - 0.0420T)/(912.55 - 0.2331T) \quad [14]$$

The temperature dependence of the mole fraction of H required for reduction of FeO (*i.e.* n *vs* T) at atmospheric pressure is shown by the dotted curve in Figure 5. The curve intersects the T axis (*i.e.* $n = 0$) at 1758 K (1485 °C), which implies that pure H_2 alone can reduce FeO at temperatures higher than 1758 K (1485 °C). At temperatures lower than 1758 K (1485 °C), H is required for reduction. The required H increases with decreasing T. Even at very low T, a relatively small mole fraction (<10 pct) of H can reduce FeO. This H moves the H_2–H_2O line below the Fe–FeO line, even at low T, as shown by the dotted lines in Figure 3. Hence, H makes the reduction of FeO feasible, even at low T.

Figure 5 also contains another curve, the atomic hydrogen mole fraction obtainable in a HP at atmospheric pressure, assuming LTE.[62–64] As evident from Figure 5, the required H mole fraction for reduction of FeO is higher than that obtainable at lower temperatures.[62–64,71–74] This has important consequences, since it indicates that in an LTE process, it does not make sense to increase the temperature up to that temperature required to produce sufficient atomic hydrogen, since (i) H_2 is able to reduce FeO at these higher temperatures; (ii) the boiling points of iron and its oxides are around 2500 K (2227 °C) and most of the traditional plasma processes are heterogeneous (solid–plasma and liquid–plasma); (iii) the equilibrium dissociation temperature of H_2 (~3500 K (3227 °C)) is much higher than the boiling points of iron and its oxides:[11] and (iv) no studies of reduction of FeO in homogeneous processes (*i.e.*, by dissociative reduction mechanisms) have been reported.[11]

However, it is important to note that the limitations of high temperature do not rule out thermal plasma processes for reduction of FeO. First, deviations from LTE can occur in thermal plasma processes, leading to anomalously high atomic hydrogen densities at low temperatures, as will be discussed in Section V–B. Further, rovibrationally excited hydrogen molecules, which are produced in LTE plasmas at relatively low temperatures, favor reduction of FeO, as will be considered in Section V–C.

Finally, homogeneous processes for iron oxide reduction are still an open possibility. High-temperature thermal plasma reduction processes using the dissociative reduction mechanism have thermodynamic and kinetic advantages.[11,65,75] They are particularly useful for refractory oxides, whose dissociation temperatures are high [~4500 K (4227 °C)].[11] At 4500 K (4227 °C), oxygen and water are completely dissociated. In dissociative reduction, the reduction process starts with the formation of metal and oxygen atoms. Then, during a quenching stage, oxygen atoms recombine with the reducing agent, thereby preventing the metal atoms from recombining with oxygen, and allowing effective metal production. The equilibrium dissociation temperature of FeO, as calculated from Eq. [14], is 4053 K (3780 °C), which is relatively low. At this temperature, water and oxygen are largely, but not completely, dissociated. Therefore, the quenching stage will not be as efficient as for refractory oxides, but nevertheless dissociative reduction of iron oxide is feasible.

1. *Effects of pressure and temperature*

ΔG° depends on the pressure P as well as temperature T. As a result, the dependence on pressure of the dissociation of hydrogen has to be considered. The ΔG° for dissociation ($H_2 = 2H$) is given by

$$\Delta G^{\circ} = -RT \ln K_D, \quad [15]$$

where the equilibrium constant for the dissociation reaction, K_D, can be written as

$$K_D = \frac{P_H^2}{P_{H_2}} = \exp\left(\frac{-\Delta G^{\circ}}{RT}\right) \quad [16]$$

Let α_D be the degree of dissociation, defined as the ratio of the number of dissociated hydrogen molecules (n_D) to the number of hydrogen molecules initially present (n_0). In equilibrium, the number of moles of H_2 is given by $n_0(1-\alpha_D)$, and the number of moles of H by $2n_0\alpha_D$.

The mole fractions of H and H_2, n and N, respectively, can be expressed, respectively, as

$$n = \frac{2\alpha_D}{1+\alpha_D} \quad [17]$$

$$N = \frac{1-\alpha_D}{1+\alpha_D} \quad [18]$$

Assuming the ideal gas law is obeyed,

$$K_D = \frac{P_H^2}{P_{H_2}} = \frac{n^2}{N} = P\frac{4\alpha_D^2}{1-\alpha_D^2} \quad [19]$$

$$\alpha_D = \sqrt{\frac{K_D}{4P+K_D}} \quad [20]$$

$$n = \frac{2\sqrt{K_D}}{\sqrt{K_D}+\sqrt{4P+K_D}} \quad [21]$$

Equation [21] contains all parameters for determining the atomic mole fraction as a function of P, at constant T. For the two extremes of pressure, *i.e.* $P \to 0$ and $P \to \infty$, we obtain $n \to 1$ and $n \to 0$, respectively. In other words, the mole fraction of H decreases with the increase in pressure.

An alternative expression for α_D was derived by Capitelli *et al.*[72] under the following assumptions: (a) The gas is ideal, (b) the standard enthalpy at 0 K (−273 °C) is approximated by the bond dissociation energy (D), and (c) the standard entropy is independent of T. Based on these assumptions, Capitelli *et al.* obtained

$$K_D = \exp\left(\frac{-\Delta G^\circ}{RT}\right) = \exp\left(\frac{-D}{RT}\right)\exp\left(\frac{\Delta S^\circ}{R}\right) = A\exp\left(\frac{-D}{RT}\right) \quad [22]$$

where $A = \exp\left(\frac{\Delta S^\circ}{R}\right)$ is a constant. Using Eq. [20], this gives

$$\alpha_D = \sqrt{\frac{A}{4P}}\exp\left(\frac{-D}{2RT}\right) \quad [23]$$

The mole fraction, n was calculated for different pressures using published ΔG° data and Eqs. [18] and [23][76]; the results are presented in Figure 6, which gives results for different temperatures, and Figure 7, which gives results for different pressures. The values obtained are compared with those obtained from Eq. [17] using α_D from Eq. [23] (*i.e.*, from the work of Capitelli *et al.*[72]), and show excellent agreement. As evident from Figures 6 and 7, n increases with the decreasing pressure and the increasing temperature. This observation is in accordance with LeChatelier's principle. As there is an increase in volume, during atomization (2 moles of H produced from 1 mole of H_2), the decrease in pressure favors the reaction in the forward direction. So, more H is produced at reduced pressure.

In earlier work on reduction of metal oxides by low-temperature HP,[11–14] although the fraction of H could not be measured, the intensity of the H_α lines of a microwave HP was obtained from the optical emission spectra for different pressures. The variation of intensity of H_α line with change of pressure is shown in Figure 8. Assuming that intensity of H_α line increases with the atomic hydrogen concentration, the observed trend,

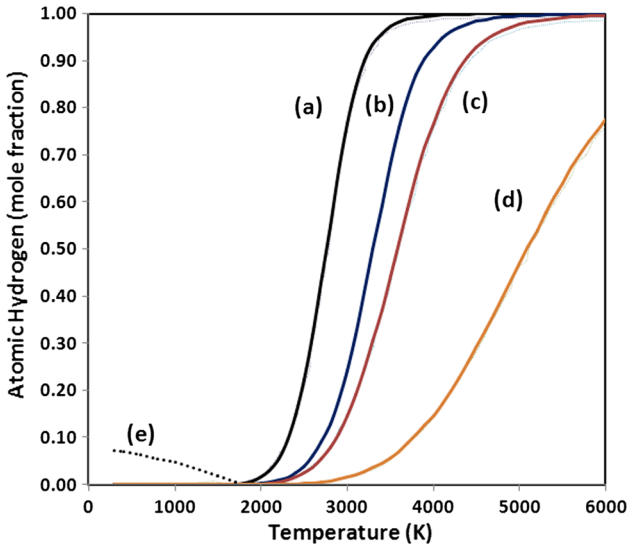

Fig. 6—Dependence of mole fraction of atomic hydrogen on temperature for different pressures: (*a*) 0.01 × 10^5 Pa (*b*) 0.1 × 10^5 Pa, (*c*) 1 × 10^5 Pa, and (*d*) 100 × 10^5 Pa. The dotted lines show the results obtained using α_D from Capitelli *et al.*[72] Curve (*e*) shows the mole fraction required for reduction of FeO.

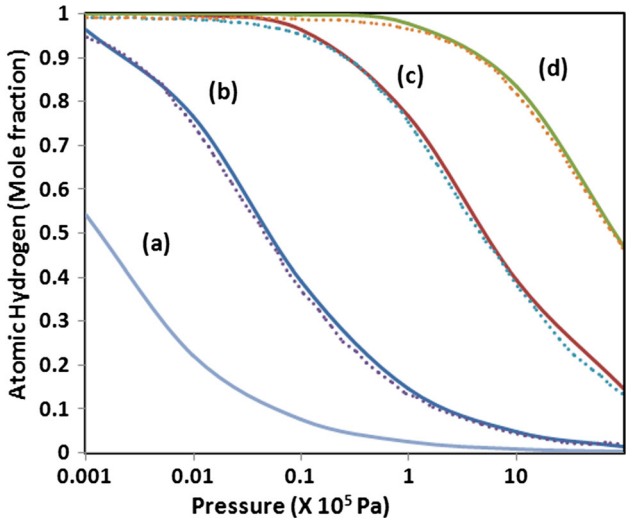

Fig. 7—Atomic hydrogen *vs* pressure at different constant temperatures (*a*) 2500 K (2227 °C), (*b*) 3000 K (2727 °C), (*c*) 4000 K (3727 °C), and (*d*) 5000 K (4727 °C). The dotted lines show the results obtained using α_D from Capitelli *et al*[72]

decreasing n with increasing pressure, is in agreement with the results shown in Figure 6.

B. *Role of Ionic Hydrogen*

In addition to atomic hydrogen, atomic hydrogen ions (H^+) are also produced in HPs; molecular ions (H_2^+ and H_3^+) can also be produced, although these have low densities in LTE. Figure 1 shows the number density of H^+ in an atmospheric-pressure HP in LTE. It can be seen that approximately half the atoms are ionized at a temperature of about 15,000 K (14,727 °C), and that the density of H^+ is very low for temperatures below about 7000 K (6727 °C).

The reduction potentials of the hydrogen ions are much higher than those of the neutral species. Zhang *et al.*[77] listed the principal chemically active species in HP at moderate pressures as H, H^+, H_2^+ and H_3^+. The $\Delta G°$ values for H_2O generated from reactions of different hydrogen species with oxygen were given in Reference 11 The reduction ability for these species varies in the order $H^+ > H_2^+ > H_3^+ > H$.[11,78] Zhang *et al.*[78] also reported the free energies for reduction of hematite (Fe_2O_3) by different chemically active species present in HP. From their reported data, $\Delta G°$ values for reduction of FeO by various chemically active species were calculated and are also presented in Figure 9.

The temperatures at which H^+ is produced in LTE are significantly higher than the boiling point of both iron and iron oxides [~2500 K (2227 °C)]. In plasma metallurgy, homogeneous reactions do not dominate unless the processed material (FeO in this case) is also in the gas or plasma state. However, iron ore reduction in practical systems takes place mainly in the solid or liquid state. Nevertheless, hydrogen ions can also play an important role in heterogeneous processes, since the polarity of the interface between the plasma and the condensed FeO charge plays a vital part in the reduction process, as we discuss in the next subsection.

C. *Role of the Polarity of the Charge/Melt*

Most studies of the reduction of iron oxide by HP have been carried out in heterogeneous systems, where the hydrogen gas is in the plasma state but the iron oxide remains in the solid[13,14,77,78] or liquid phase.[79–92] The reduction at this interface depends on the number of particles reaching the interface. HP contains both heavy positively charged particles, and light negatively charged electrons. According to statistical thermodynamics $\left(\frac{1}{2}mv^2 = \frac{3}{2}kT\right)$, the velocity of the electrons is much higher than the velocity of ions. Thus, the electron flux to the interface dominates, and a negative potential develops. This negative potential then starts repelling electrons and attracting positive ions until the charge is balanced; *i.e.*, the interface attains quasi-neutrality. This phenomenon is localized in a narrow region called the plasma sheath.

When a polarity is applied to a surface, it will repel like-charged particles and attract particles of opposite polarity. If the surface of FeO is given a positive polarity, electrons are attracted, and molecular and atomic hydrogen ions are repelled.[77,78,80,86] As a consequence, electrons form a narrow region at the interface, and the particles reaching the reduction interface are neutral atoms and molecules. Conversely, a negatively charged surface will repel electrons and attract positive molecular and atomic ions. As noted in Section III–B, these positively charged ions have very high reducing ability.

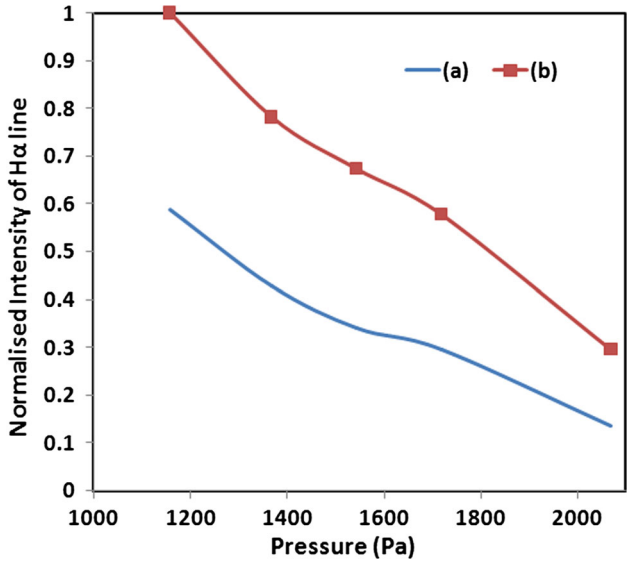

Fig. 8—Variation of intensity of the H_α line with pressure in a microwave hydrogen plasma for two powers: (*a*) 600 W and (*b*) 750 W.

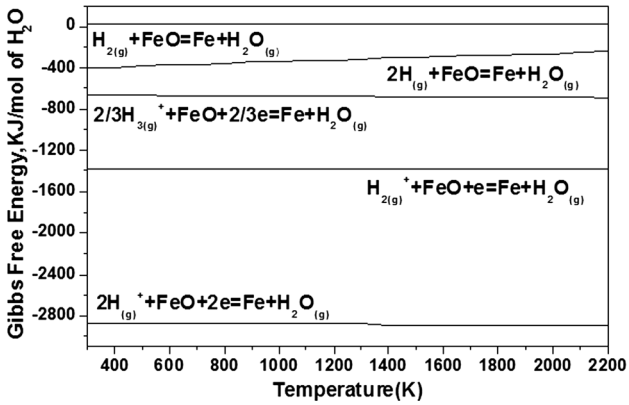

Fig. 9—$\Delta G°$ – T curves for H_2O for different chemically active hydrogen species.

Dembovsky *et al.*[93] examined the thermodynamics with and without an externally applied polarity in the case of FeO reduction by HP. They calculated $\Delta G°$ with and without polarity by taking into account the concentration of different species present in the HP; their results were presented in Reference 11 It was found that the application of positive polarity to the previously neutral FeO surface reduces the probability that a reaction will proceed as intended. A negative polarity decreases $\Delta G°$ by a factor of around six, indicating that the likelihood of the reduction reaction proceeding is extremely high, and that the equilibrium is shifted to the product side. For example, a positive charge alters the standard heat of reaction by +62.7 kJ/mol, but a

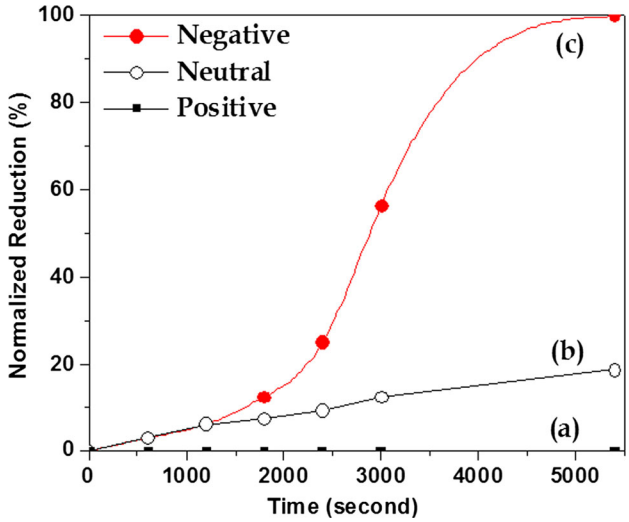

Fig. 10—Relative reduction of tablets of Fe_2O_3 by a DC pulsed hydrogen plasma reduction for (*a*) an applied positive charge, (*b*) no applied charge, and (*c*) an applied negative charge.

negative charge on the surface alters it by −1999.4 kJ/mol, relative to the neutral surface.[93,94]

There is some experimental evidence for this effect. Zhang *et al.*[78] carried out HP reduction of tablets of Fe_2O_3 in a DC pulsed hydrogen glow discharge at 763 K (490 °C) and 1500 Pa. The tablets were reduced with and without an applied polarity. The results are shown in Figure 10. There was no reduction when a positive polarity was applied to the sample. Reduction took place when the sample was neutral, and the extent of reduction increased by a factor of about six when the surface was negatively charged. This is discussed in more detail in Section VI–A.

IV. THERMOPHYSICAL PROPERTIES OF HYDROGEN PLASMAS

An effective heterogeneous reduction process requires that the HP interacts with the iron oxide over a large interfacial area. The thermophysical properties of the plasma, which include the thermodynamic and transport properties, are important because they strongly influence the momentum, heat, and mass transfer, and hence the reduction process. As the iron and its oxides vaporize at relatively low temperatures, below 2300 K (2027 °C), and their gas-phase dissociation temperatures are also low, we have limited our discussion of these properties to temperatures below 6000 K (5727 °C). Also, although we use the term HP, generally the plasma that is employed in practice includes a large proportion of argon. Argon is added to optimize the transport properties to ensure that the required arc properties are obtained, as discussed below. Therefore, we consider in detail the effect of hydrogen addition to argon. The characteristics of argon–HPs over a wide temperature range, from 300 K to 30 000 K (27 °C to 29 727 °C), have been discussed in detail in the literature.[3–5,95,96]

A. *Calculation of Thermophysical Properties*

The thermophysical properties are calculated assuming local thermodynamic equilibrium (LTE). As noted in Section II, this assumption is satisfied in the central regions of a thermal plasma; deviations may occur in the edge region, or close to the electrodes.

The composition of the plasma is calculated by minimizing the Gibbs free energy of the gas mixture, under the constraint of charge neutrality. The Gibbs free energy for a gas mixture is

$$g = \sum_i \mu_i N_i, \qquad [24]$$

where N_i is the number of moles, and μ_i is the chemical potential of species i.

The chemical potential of an ideal gas is

$$\mu_i(T,P) = \mu_i^0(T) + RT\ln(n_i/n) + RT\ln(P/P_0), \qquad [25]$$

where R is the ideal gas constant; T is the temperature; n_i is the number density of species*i*; n is the total number density; P is the pressure and $P_0 =$ 1 bar; and $\mu_i^0 = H_i^0 + TS_i^0$ is the chemical potential of species i in the standard state (*i.e.*, at atmospheric pressure); H_i^0 and S_i^0 are, respectively, the standard-state enthalpy and entropy per mole. To calculate the composition of a mixture of hydrogen and argon, the required data are therefore the standard-state chemical potentials of the species that may be present, including H_2, H, H_2^+, $H+$, Ar, Ar^+, Ar^{2+}, and e^-. These data can be calculated from spectroscopic parameters of the species.

Once the composition of the gas mixture is known, it is a simple matter to calculate the thermodynamic properties. For example, the mass density is given by

$$\rho = \sum_i n_i m_i, \qquad [26]$$

where m_i is the mass of species i. The specific enthalpy is given by

$$h = \frac{1}{\rho}\sum_i n_i m_i h_i, \qquad [27]$$

where h_i is the enthalpy per unit mass of species i, and the specific heat at constant pressure is given by

$$c_p = \left.\frac{dh}{dT}\right|_P \qquad [28]$$

Calculation of the transport coefficients, such as viscosity, thermal conductivity, and electrical conductivity, is more complicated, since they depend on the collision cross-sections of each of the species with one another, and must be calculated from the kinetic theory of gases. The usual method of calculation of the transport coefficients is the Chapman–Enskog method,[97] which is an approximate method of solution of the Boltzmann equation. The collision cross sections are integrated over a Maxwellian distribution of velocities to give "collision integrals". In plasmas, it is necessary to consider interactions between pairs of neutral particles, between pairs of charged particles,

between neutral particles and ions, and between neutral particles and electrons. Different procedures are used for each type of interaction; details are given by, for example, Boulos *et al.*[98] Some simplifications are possible due to the very large mass difference between electrons and the heavy species.[99]

The expressions for the transport coefficients are too complicated to reproduce here; instead we present approximate expressions which indicate the dependence on temperature and composition.[100]

The viscosity depends on the mass of the heavy species m_h, the temperature T and the collision integrals for interactions between pairs of heavy species Ω_{hh} according to

$$\eta \sim \frac{\sqrt{m_h T}}{\Omega_{hh}} \quad [29]$$

The electrical conductivity depends on the electron density n_e and the collision integrals for interactions between electrons and heavy species Ω_{eh} according to

$$\sigma \sim \frac{n_e}{\sqrt{T} n \Omega_{eh}} \quad [30]$$

The thermal conductivity has four different components. The translational thermal conductivity due to the motion of heavy species is given by

$$k_h \sim \frac{c_p}{\Omega_{hh}} \sqrt{\frac{T}{m_h}} \quad [31]$$

In addition, there is translational conductivity due to the motion of electrons, which is small at the relatively low temperatures of interest here, the internal thermal conductivity due to the transport of internal energy of the species (such as the vibrational energy of molecules), and the reaction thermal conductivity. The latter refers to transport of the heat of dissociation of molecules, and heat of ionization of molecules and atoms, and tends to dominate at the temperatures at which dissociation and ionization reactions occur.

B. *Enthalpy and Specific Heat*

The enthalpy and specific heat are thermodynamic properties that substantially affect the heat content of plasma, and hence the reduction of iron oxides to metallic iron, which are endothermic reactions. Further, as discussed below, they influence the constriction of arc plasmas, and therefore the interfacial area between the arc and the charge material.

The enthalpy and specific heat values of argon–HPs with 10, 20, 30, 40, and 50 pct hydrogen are shown in Figures 11 and 12, respectively.[101] As shown in figures, the enthalpy and specific heat values are the lowest for pure argon (shown as a dotted line), and the enthalpy increases approximately linearly with the temperature. The addition of hydrogen increases the heat content and specific heat of plasma, the increase being approximately proportional to the proportion of hydrogen added, as expected from Eqs. [27] and [28]. The enthalpy and specific heat start to increase abruptly at temperatures

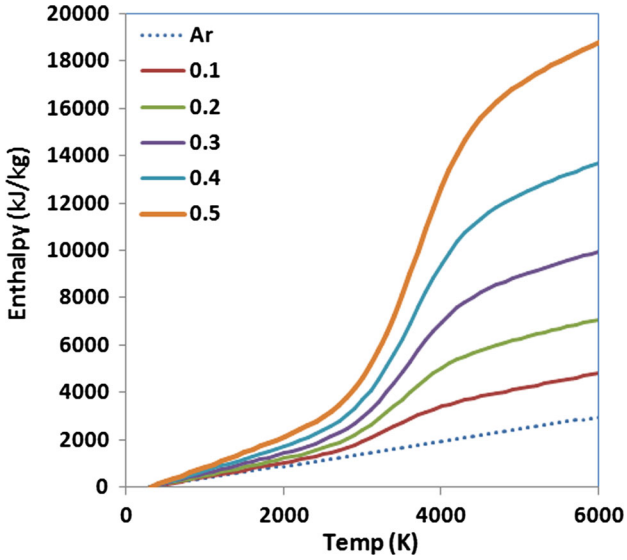

Fig. 11—Temperature dependence of enthalpy of atmospheric-pressure LTE plasmas in argon, and argon–hydrogen mixtures with mole fractions from 0.1 to 0.5 hydrogen.

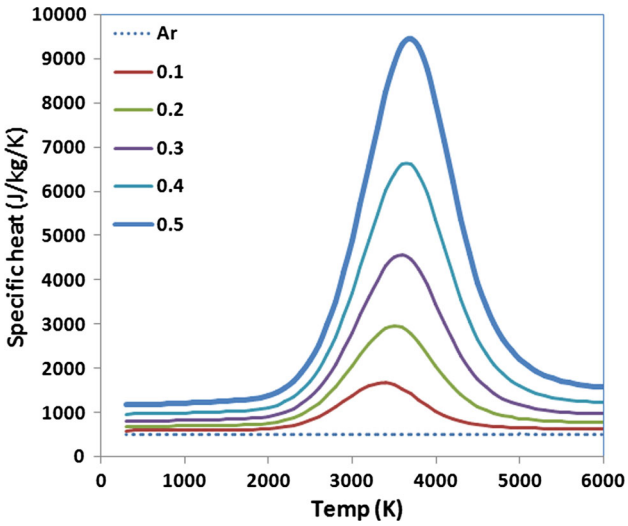

Fig. 12—Temperature dependence of specific heat of atmospheric-pressure LTE plasmas in argon, and argon–hydrogen mixtures with mole fractions from 0.1 to 0.5 hydrogen.

from around 2000 K (1727 °C) due to dissociation of hydrogen molecules. The large peak in the specific heat for mixtures containing hydrogen is centered at around 3500 K (3227 °C), at which temperature, hydrogen is approximately 50 pct dissociated (see Figure 1). This heat of dissociation remains stored inside the plasma, and is delivered during recombination of atomic hydrogen at the plasma–oxide interface.[80] This heat favors the reduction of FeO; hence the presence of hydrogen assists reduction thermally as well as chemically.

Ionization of hydrogen and argon atoms is not significant until temperatures above 6000 K (5727 °C), so no corresponding peaks in specific heat are apparent in Figure 12.

The constriction of an arc can be estimated from specific enthalpy using the relationship[102]

$$IV_z \sim \rho_z h_z v_z A \qquad [32]$$

which approximates the total power flowing toward the lower electrode (*i.e.*, the charge material in steelmaking applications) in a DC arc by the product of the arc current I and the potential difference V_z between the upper electrode and the plasma at the axial position z. This power is then equated to the rate of enthalpy flow, given by the product of the density ρ_z, the enthalpy h_z, the flow speed v_z at position z, and the cross-sectional area of the arc A.

From the above equation, it is clear that, for a given arc power IV_z, an increase in the product of density and enthalpy (which has units of energy per unit volume) will lead to a decrease in area (*i.e.* constriction of the arc), if the flow velocity does not change. This has been termed the *thermal pinch effect*.[102,103]

Hydrogen has a large specific enthalpy (enthalpy per unit mass). Despite its low atomic mass, the product of enthalpy and density is larger than that of argon, leading to a more constricted arc. Also, as will be discussed in Section IV–D, the flow velocity is larger in hydrogen arcs, further increasing the constriction according to Eq. [32]. Adding argon to hydrogen decreases the product of enthalpy and density, and the flow velocity, therefore gives a less constricted arc. This increases the interfacial area at the interface between the arc and the charge material, which facilitates the transport of heat from the plasma to the full surface area of the charge material. This favors the reduction process, so argon is generally added to HP.

C. *Thermal Conductivity*

The thermal conductivity of argon, and argon–hydrogen mixtures, is shown in Figure 13. The thermal conductivity of argon increases with temperature. With the addition of hydrogen, the thermal conductivity increases significantly. These trends are as expected from Eq. [31], since the heavy-species translational thermal conductivity dominates at low temperatures. When hydrogen is present, there is a large peak centered at around 3500 K (3227 °C), which is due to the reaction conductivity associated with the dissociation of hydrogen molecules. The presence of even a small amount of hydrogen makes a strikingly large difference to the thermal conductivity, particularly at temperatures at which hydrogen is dissociated.

Since plasma temperatures close to the charge material are typically below about 5000 K (4727 °C), the presence of hydrogen leads to a very strong increase in conductive heat transfer to the charge material.[101] This has been exploited in arc welding, and is clearly of strong benefit in liquid-HP reduction processes.

D. *Viscosity and Plasma Flow Velocity*

Argon is much heavier than hydrogen. From Eq. [29], we therefore expect that the viscosity of argon is much greater than that of hydrogen. However, it is interesting to note that the addition of 25 pct hydrogen to argon plasma does not significantly affect the viscosity.[63]

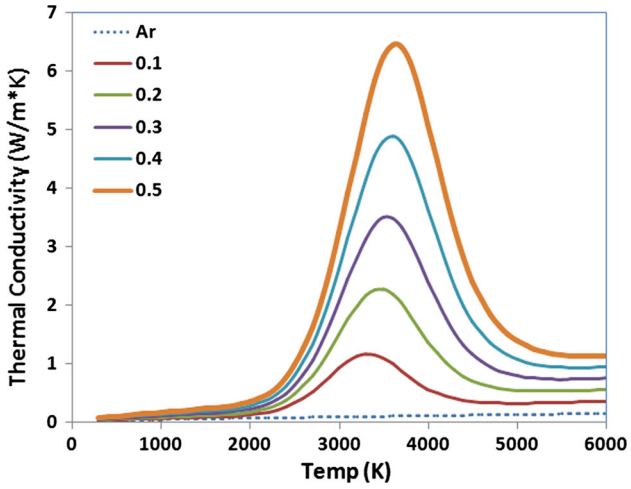

Fig. 13—Temperature dependence of thermal conductivity of atmospheric-pressure LTE plasmas in argon, and argon–hydrogen mixtures with mole fractions of 0.1 to 0.5 hydrogen.

Since the reduction of iron oxide occurs at the interface between the plasma and the charge material, the transport of the active species in the plasma toward the interface is important, so plasma velocity plays an important role in the hydrogen plasma smelting reduction (HPSR) process. The higher the velocity, the greater the convective heat transport and the greater the flux of active species toward the interface.

Figure 14 shows the calculated plasma axial velocity in Ar and H_2 arc plasmas. It is clear that the increase in the axial velocity for the hydrogen arc is dramatic. The voltage of the HP is 3 times larger, but the axial velocity increases by around 20 times near the cathode tip. Eq. [32] shows that this increase in velocity further increases the constriction of the arc. Thus, both the higher values of the product of density and enthalpy, and the higher velocity, lead to a more constricted arc when hydrogen is present.

The higher velocity is a consequence of two factors. The main factor is that the constriction of the arc leads to the increase of current density near the cathode and consequently to an increase in the $\mathbf{j} \times \mathbf{B}$ or Lorentz force, where $\mathbf{j}$ is the current density in the arc, and $\mathbf{B}$ is applied magnetic field. The Lorentz force tends to squeeze the arc and increase the pressure on the arc axis. This pressure is the driving mechanism for the convective flow in the arc as it causes a strong axial flow away from the electrode toward the melt (pinch effect).[102,103] The second factor is the lower viscosity of hydrogen arcs. Viscosity is a measure of the transport of momentum transverse to the flow direction; *i.e.*, the spreading of the flow. Lower viscosity therefore implies that the flow velocity remains high near the axis, with the momentum not transferred to larger radii.

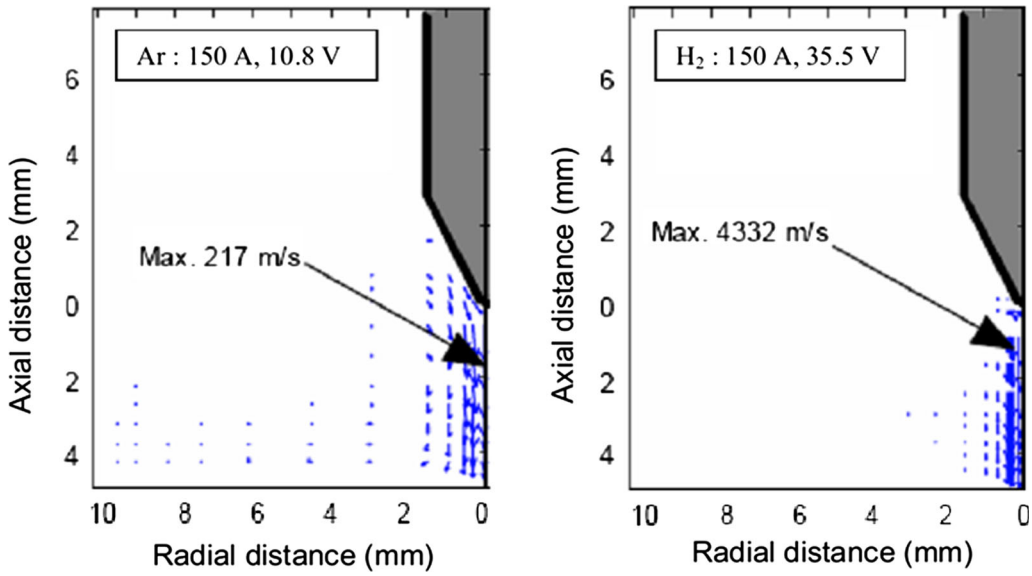

Fig. 14—Calculated velocity fields for tungsten-inert-gas welding arcs in Ar and H_2, for an arc current of 150 A.[103] Reproduced from Ref. [103] by permission of Taylor & Francis Ltd, http://www.tandfonline.com.

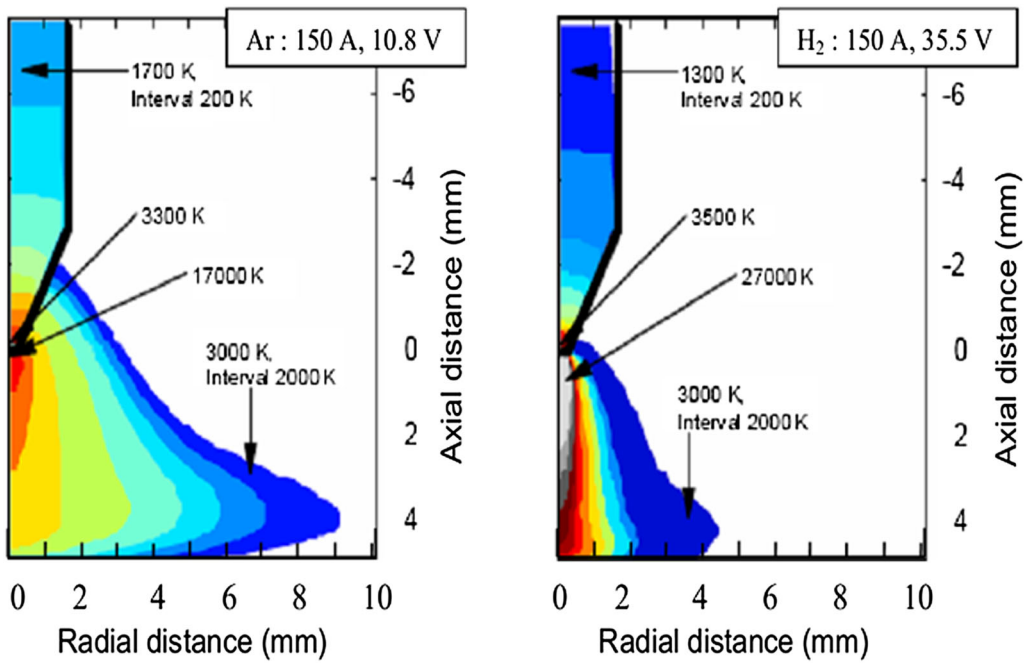

Fig. 15—Temperature fields for arcs in Ar and H_2, for the same conditions as Fig. 14.[103] Reproduced from Ref. [103] by permission of Taylor & Francis Ltd, http://www.tandfonline.com.

E. *Coverage Area*

Badr[80] studied the HPSR of iron oxide. He reported that addition of hydrogen increases the arc temperature and constricts the arc. This is in accordance with our discussion in Section IV–A. Murphy *et al.*[103] reported the temperature distribution of Ar and H_2 arcs near the melt surface. As shown in Figure 15, the argon plasma had a wider coverage area, even though the voltage and therefore the arc power was one-third that of the HP. This leads to a higher heat flux density, but the arc covers a smaller area, which is problematic for reduction of the charge material.

The arc constriction reduces the area of contact of the plasma with the molten FeO. While this can increase the rate of reduction near the arc axis, the rate of reduction averaged across the interface between the charge material and the plasma is decreased. Argon addition increases the coverage area, thereby increasing the

average rate of reduction. Due to the advantages of argon addition, most of the HP reduction processes of iron ore have been carried out with Ar-H_2 plasmas.

V. KINETICS AND NONEQUILIBRIUM PROCESSES

In Sections III and IV, we have considered HP reduction of iron ore under equilibrium conditions. In Section III, we emphasized the importance of vibrationally excited hydrogen molecules, and atomic and ionic hydrogen, noting that reduction of FeO to Fe by ground-state hydrogen molecules was not thermodynamically favorable. In Section IV, we discussed the thermophysical properties of equilibrium HP, and how these influenced the reduction of iron oxides.

In this section, we extend the discussion to consider chemical reaction kinetics and deviations from thermal and chemical equilibrium. These factors are critical in understanding real reduction processes, since (1) reaction kinetics determine the rate of chemical reactions, and (2) in reality, even thermal plasmas are never fully in equilibrium. We consider deviations from equilibrium in both thermal and nonequilibrium plasmas. Relevant experimental results that have been obtained using nonequilibrium plasmas are presented in Section VI–A. By far the majority of experimental results have been obtained using thermal plasmas, and these are considered in Section VI–B.

A. *Reaction Kinetics*

As the reduction of iron oxide proceeds, a layer of metallic iron forms at the interface between the iron oxide charge and the HP. If the diffusion of hydrogen in the metal layer is not the rate-limiting step, then the rate of the reduction process is determined by the nature of the excited hydrogen species present in the HP, and their concentration adjacent to the surface of the charge. For a reduction reaction to occur, the high-energy molecules of the reductant and the substance being reduced must first interact at the reduction interface so as to overcome the activation barrier of reduction. Depending on their internal energy, the corresponding rate coefficients can vary over several orders of magnitude.[104] In the present context,[11–14,77–92] the high-energy active species from the HP interact with the iron oxide surface to overcome the activation barrier of the reduction reaction. The lowering of activation energy and the faster kinetics of reduction of iron oxide by HP, in comparison to neutral H_2 and to other reducing plasmas, has already been reported in the literature.[11–14,80]

Rajput *et al.*[13,14] carried out solid-state reduction of hematite at different H_2 pressures, using neutral H_2 and HP, in a microwave HP reactor. The activation energy decreased from a value of 45 to 20 kJ/mol in the HP. This decline in activation energy was tentatively attributed to rovibrationally excited hydrogen molecules, denoted as H_2^*. Rajput *et al.* obtained HP at different combinations of microwave powers and pressures, *i.e.*, at different microwave power densities (MWPDs). Based on the distribution of HP species in a microwave-assisted low-temperature HP reported by Hassouni *et al.*[105] for similar conditions, it is assumed that the plasma consists of 2 pct H, 8 pct vibrationally excited H_2^* ($v = 1$ level), with the remaining 90 pct being ground-state H_2. The HP energy calculated for this composition is 21.5 kJ/mol. Using this energy and ΔG° of the reactants and products, the activation energy for reduction of Fe_2O_3 was calculated and is shown in Figure 16. The decrease in the activation energy for the HP (25 kJ/mol) agrees reasonably well with the calculated HP energy of 21.5 kJ/mol.

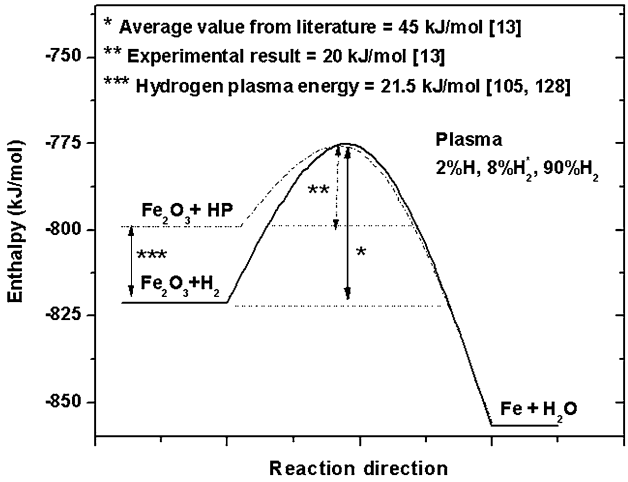

Fig. 16—Reduction in activation energy for reduction of Fe_2O_3 when molecular hydrogen is replaced by a hydrogen plasma.

Other authors[104,106] reported that H_2^* molecules stimulate the chemical processes through their surface dissociation and diffusion of H into the crystal structure to the reduction interface, thereby giving rise to faster reduction kinetics. The role of H_2^* in HP has been emphasised in the literature[11,104,106] and is discussed in detail in Section V–C.

Lowering of the activation energy has also been reported for liquid iron oxide. Badr[80] carried out the reduction of hematite in the liquid state by neutral H_2 and HP, and reported a decrease in activation energy in the presence of plasma. This lowering of activation energy increased the rate of reduction of FeO by almost one order magnitude.[87,89,90] The authors also reported that the reduction process by HP was controlled by chemical reactions. Hence, the interfacial area between the HP and the iron oxide plays a significant role in the kinetics of reduction. Badr *et al.* also compared the reduction of iron oxide by HP with that by a CO plasma. They reported the activation energy for reduction by HP (23 kJ/mol) is 15 pct of that by CO plasma (150 kJ/mol), and that the reduction kinetics for the HP are 3.4 times faster than the CO plasma.

A schematic diagram of the activation energy profile for reduction of FeO with different hydrogen species is shown in Figure 17. Reduction of FeO to Fe by H_2 is thermodynamically feasible at high temperatures, as discussed in Section II. However, the high activation energy (denoted by E_1 in Figure 17) prevents the reduction from occurring. When H_2 molecules absorb energy to become H_2^*, their internal energy increases,

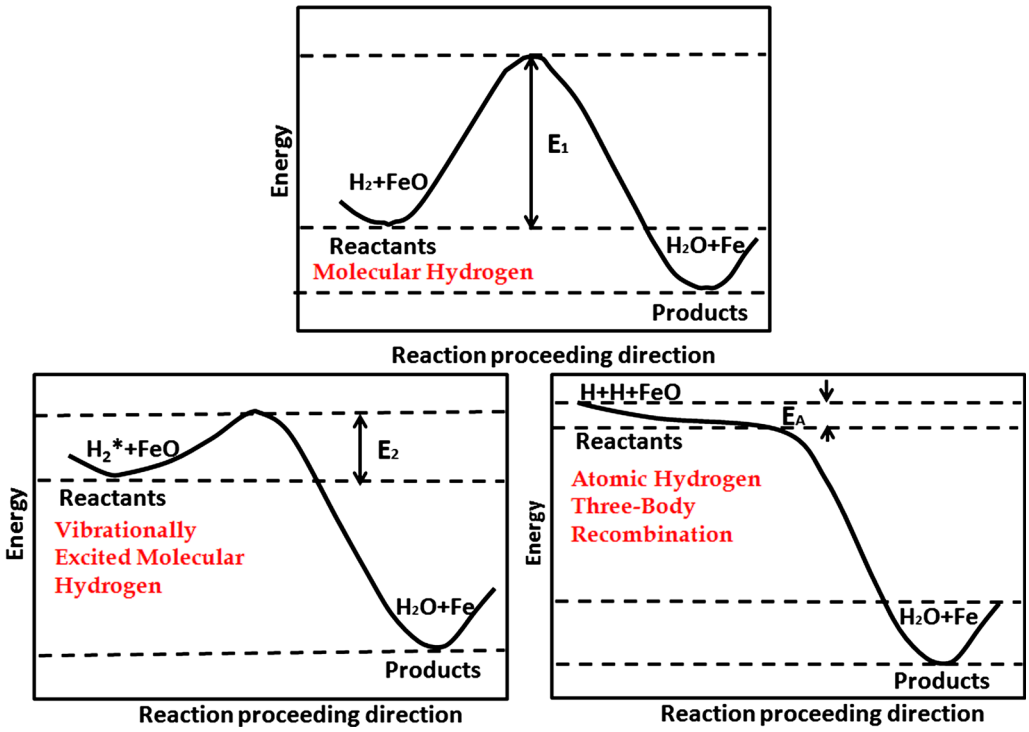

Fig. 17—Schematic diagram of the activation energy profile for reduction of FeO by different hydrogen species.

which leads to a decrease in the activation energy E_2. When the stored energy becomes significant, the activation energy (E_A) may become negative, as it does in the case of atomic H. A decrease in activation energy makes the reduction easier.[11]

B. *Deviations from Local Thermodynamic Equilibrium in Thermal Plasmas*

The composition of a HP under LTE conditions was shown in Figure 1. It can be seen from the figure that the atomic hydrogen concentration approaches zero at temperatures below about 2500 K (2227 °C). The composition is calculated assuming that reaction rates are infinitely large, so that the composition is determined by chemical equilibrium. As was noted in Section III–A, deviations from LTE can occur near the electrodes and in the fringe regions of thermal plasmas. Of particular interest in the context of iron oxide reduction are deviations from LTE due to a delayed recombination of hydrogen atoms. This can lead to a higher flux of hydrogen atoms to electrodes (for example the iron oxide charge in HP reduction).

The recombination of hydrogen atoms to form molecules is a three-body reaction:

$$H + H + M \rightarrow H_2 + M$$

where M represents any third body. Three-body reactions are relatively slow; moreover diffusion rates are high in the fringes of thermal plasmas and close to the electrodes because of the large temperature gradients. This means that the rate of diffusion of atomic hydrogen to the fringes of the plasma and to the electrodes can be much larger than the rate of recombination.

This has been demonstrated experimentally by Snyder *et al.*,[107] who used two-photon laser-induced fluorescence to measure the distribution of hydrogen atoms in an argon–hydrogen arc plasma. Comparison with the calculated distribution of hydrogen atoms indicated that the hydrogen atom density was much higher than predicted by the local temperature and LTE. Ye *et al.*[108] calculated the atomic hydrogen distribution in a thermal radio-frequency plasma taking into account the rate of the recombination reaction, and found that the atom density was much higher than predicted by LTE in the fringes of the plasma.

These results indicate that it is possible to obtain a substantial flux of atomic hydrogen to the iron oxide charge material from a thermal plasma, even though the temperature in the gas adjacent to the charge material is below the dissociation temperature of hydrogen molecules.

C. *Rovibrationally Excited Hydrogen Molecules*

We noted in Section II–A that hydrogen molecules become rotationally and vibrationally excited as temperature increases in thermal plasmas. The population of the excited states is described by the Boltzmann distribution:

$$\frac{n_{v,J}}{n} \propto \exp\left(\frac{-E_{v,J}}{k_B T}\right), \qquad [33]$$

where $n_{v,J}$ and $E_{v,J}$ are the number density and energy of the states with vibrational level v and rotational level J, n is the total number density, and k_B is Boltzmann's constant. For example, the first vibrational

level at $E_{1,0} = 0.516$eV is 1 pct occupied at the temperature of 1300 K (1027 °C), and 10 pct occupied at 2600 K (2327 °C).

Figure 18 shows the effect of vibrational excitation of H_2 on $\Delta G°$ of HP. The figure displays the variation of $\Delta G°$ for the reaction $2H_2 + O_2 = 2H_2O$, with and without different vibrational excitations. The dotted line represents the Fe–FeO line. It is observed that $\Delta G_7°$ decreases as the level of vibrational excitation v increases, with the H_2–H_2O line moving downward. Once the H_2–H_2O line moves below the Fe–FeO line, reduction of FeO becomes feasible; this is achieved even for lowest vibrational levels $v = 1$ or 2, depending on the temperature.

Practically, HP also contains other vibrationally excited hydrogen molecules with higher vibrationally excited levels ($v = 3$ to 14) and atomic H, as reported by Hassouni *et al.*[105] They studied the chemical kinetics and energy transfer of microwave HP at different powers and pressures, and hence different MWPDs, as listed in Table II. They calculated the vibrational distribution functions for all vibrational levels ($v = 0$ to 14), for various discharge conditions. Of these, only the first two lowest vibrational levels $v = 1$ and $v = 2$ are shown in Table II. These two levels have been used in the calculation of $\Delta G°$ for the Ellingham diagram, shown in Figure 19. The figure shows the $\Delta G°$ for different MWPDs, as reported in Table II. As evident from Figure 19, with an increase in MWPD, the Gibbs free energy decreases, indicating the feasibility of reduction at a lower temperature. This figure can be compared with Figure 3 of,[11] which shows a similar diagram but for HP with different fractions of atoms and no vibrationally excited molecules. It is clear that the presence of the vibrationally excited molecules significantly increases the reducing potential of the HP, allowing reduction of FeO to occur even with low levels of vibrational excitation and dissociation induced by a low MWPD.

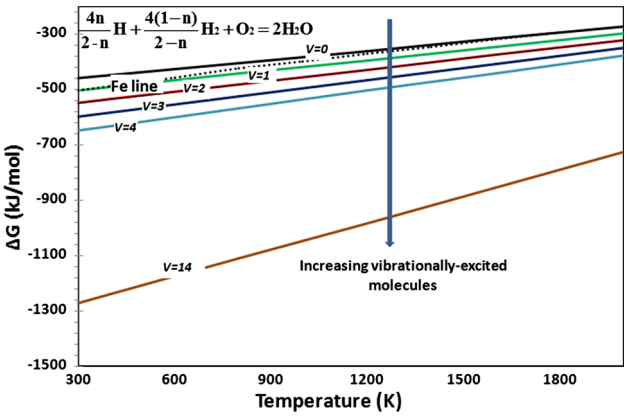

Fig. 18—Effect of vibrational excitation of molecular hydrogen on standard free energy of a hydrogen plasma. The free energy required for reducing FeO to Fe is shown by the dotted line.

As mentioned above, the calculations of $\Delta G°$ in Figure 19 have been done only for the first two vibrational levels $v = 1$ and $v = 2$. If other vibrational levels ($v = 3$ to 14) are included in the $\Delta G°$ calculation, $\Delta G°$ would decrease further.

In nonthermal HPs, it is possible to have much higher rovibrational populations than that given by the Boltzmann distribution for a given gas temperature. As noted in Section II–B., the temperatures typically follow the order $T_e > T_v > T_r \approx T_i \approx T_g$.[51,52] In typical nonthermal plasma systems, T_e is about 1 eV (~ 11 600 K (11327 °C)), while T_g is close to room temperature. This avoids the problem of overheating encountered in thermal plasmas, and traditional furnaces used for iron oxide reduction. A typical temperature distribution is shown in Figure 20.

Electrons play a critical role in energy transfer in nonthermal plasmas.[109] The hydrogen molecules gain energy from collisions with the electrons. Most of the acquired energy is stored as rovibrational excitation.[11,65,105,109,110] Hassouni *et al.*[105] reported the energy distribution to various channels in a moderate pressure microwave HP diamond-deposition reactor. The percentage power dissipation to channels, estimated from their stated values, is shown in Figure 21. Most of the energy gained by electrons from the high-frequency (HF) electric field (more than 70 pct) was transferred to the vibrational modes of H_2 through electron collisions (e–V processes). Other significant energy-transfer channels were electron-impact dissociation, gas heating (elastic collisions), electronic excitation, and ionization of H_2 and H. The power lost by electrons in electron-impact dissociation, gas heating (elastic collisions) was low compared with the energy transferred to e-V processes. The energy transferred to electronic excitation and ionization of H_2 and H always remained negligible.

Table II. Working Parameters and Atomic Hydrogen Concentration in Diamond MPACVD Reactor[105]

Pressure (Pa)	Input Microwave Power (W)	Average MWPD ($\times 10^6$ W m^{-3})	Atomic H Fraction	Vibrationally Excited ($v = 1$) H_2^* Fraction	Vibrationally Excited ($v = 2$) H_2^* Fraction
1400	300	4.5	0.01	0.0274	0.0011
2500	600	9	0.02	0.0786	0.0035
5200	1000	15	0.03	0.1001	0.0119
8400	1500	22.5	0.075	0.1265	0.0207
11000	2000	30	0.16	0.1328	0.0222

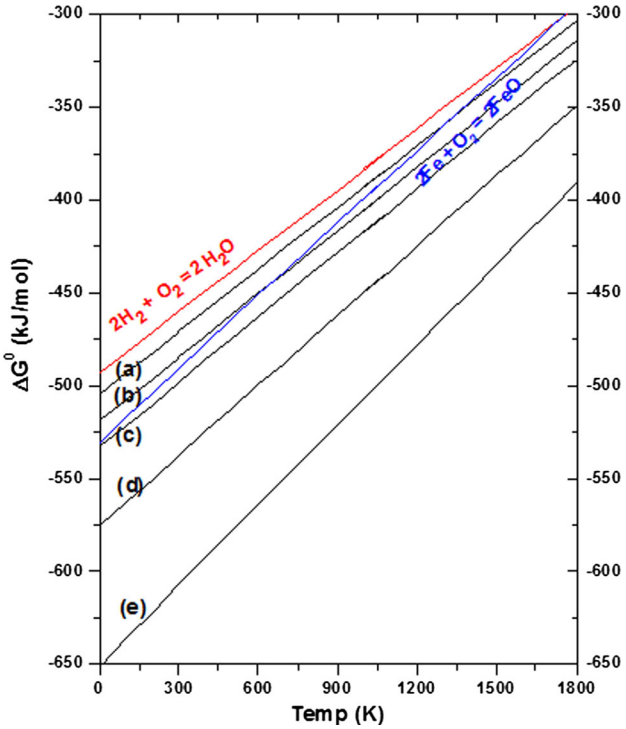

Fig. 19—The Ellingham diagram for FeO reduction and for H_2O reduction for different hydrogen plasmas compositions at MWPDs: (*a*) 3.5 × 10^6 W m^{-3}, (*b*) 9 × 10^6 W m^{-3}, (*c*) 15 × 10^6 W m^{-3}, (*d*) 22.5 × 10^6 W m^{-3}, and (*e*) 30 × 10^6 W m^{-3}.

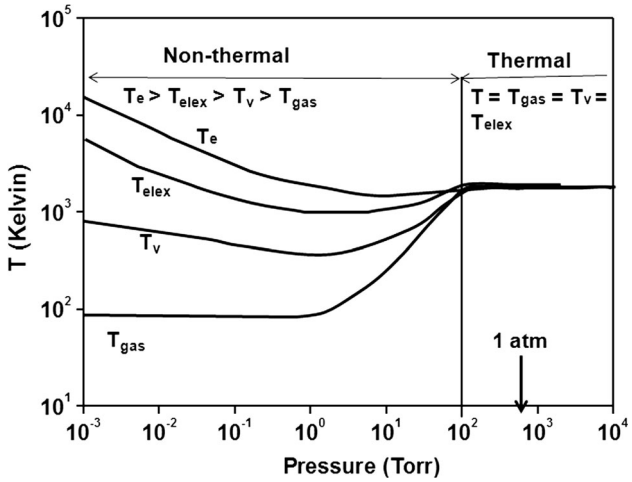

Fig. 20—Temperatures prevailing in hydrogen plasmas at pressures.

In atomic gases, such as Ar and He, the gas temperature increases when electrons collide with atoms, because of electron–translational (e–T) energy transfer. But in molecular gases, electrons transfer energy to rotational and vibrational modes. Typical rotational energy steps are small (the first rotational level of hydrogen is at 0.015 eV). However, vibrational energy levels are comparable to typical values of T_e (the first vibrational level of hydrogen is at 0.516 eV).[111] The

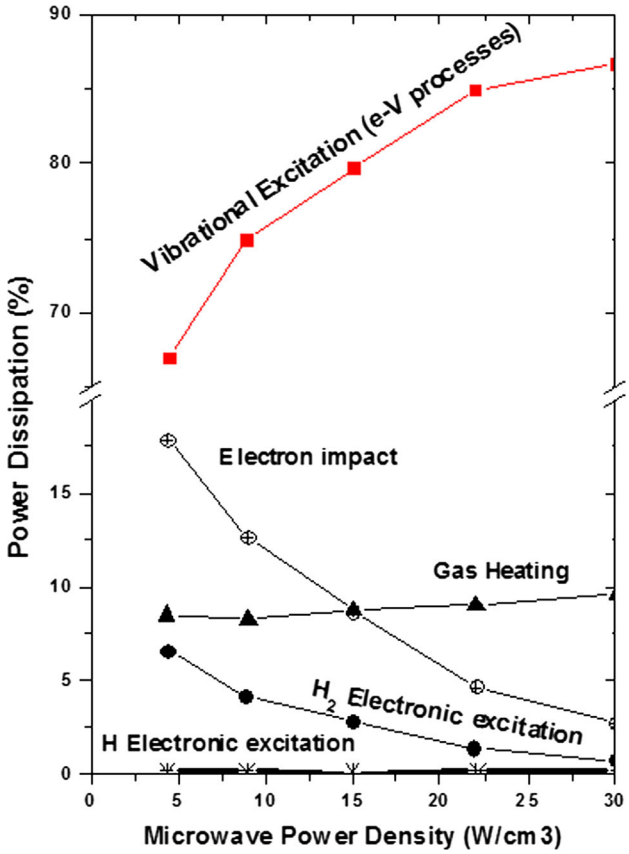

Fig. 21—Power dissipation to channels in microwave hydrogen plasma reactor, using data from Ref. [105].

majority of electrons transfer their energy to vibrational energy, e–V, of hydrogen gas molecules by a step-by-step process.[65] The molecules can maintain this energy for a long time (10^{-3} – 10^{-2} s) until the accumulated vibrational energy reaches the dissociation threshold.[112]

There is a great deal of experimental evidence for elevated values of T_v while T_g remains low. For example, Staack *et al.*[51] investigated a DC normal hydrogen glow discharge at a pressure somewhat below atmospheric (40 kPa). They reported a T_v of 4956 K (4683 °C) while T_g was 754 K (481 °C). Shimizu *et al.*[113] obtained T_v in the temperature range 7600–8600 K (7327–8327 °C) while keeping a low T_g (638–962 K (365–689 °C) in a microwave HP at 133–400 Pa and 600 W. There are many other reports of significant increases in T_v.[114–120]

The vibrational temperature in nonthermal plasmas can be very high, significantly increasing the hydrogen dissociation rate.[105,121–128] The thermodynamic equations for multi-temperature nonthermal plasmas have been derived by several authors.[98,129–140] The internal partition function of H_2 (vibrational and rotational) has been calculated at T_g by Capitelli *et al.*[71,72,125,132–134] for each of 14 vibrational levels, up to the dissociation limit. Capitelli *et al.*[72] have also calculated the partition function of H.

D. *Transfer of Energy from the Plasma to the Reaction Interface*

There are several mechanisms by which energy is transferred from a plasma to a surface. In all cases, thermal conduction is important, since the plasma temperature is higher than that of the surface. In the case of a transferred arc plasma, an additional mechanism is the transfer of energy by electrons. If the surface is the anode (which is normally the case for metallurgical processes), the energy flux can be approximated as[141]

$$H = j\varphi_w - k\nabla T, \quad [34]$$

where j is the current density, φ_w is the work function of the surface, k is the thermal conductivity, and T is the temperature.

For the case of a molecular-gas plasma, such as a HP, there are also important reactive heat-transfer mechanisms from rovibrationally excited molecules and atoms, which we consider here.

Relaxation of vibrationally excited states is relatively slow in the gas phase, particularly at low gas temperatures, for which the collision rate is low. The main mechanisms are V–V or V–T relaxation, which refer, respectively, to transfer of energy to the vibrational excitation of another molecule, and transfer to the translational energy of another species. V–T relaxation is faster than V–V relaxation in the gas phase, but V–T relaxation at the reduction interface is much faster again.[65,142]

The high rate of V–T relaxation at the surface, and the low rate of relaxation in the gas phase, are important factors in reduction of FeO in a HP process. They favor the transfer of the vibrational energy of hydrogen molecules to the reduction interface, increasing the energy of the reacting species at the reduction interface. This decreases the activation barrier, increasing the reaction rate.[13,65] Since the reduction of FeO is endothermic, the energy is important in ensuring that the reduction is feasible at low temperature in HP.[13] The transfer of energy stored in the plasma by rovibrationally excited molecules is in fact important for a broad range of applications.[110] The phenomenon is called nonthermal surface heating.[65] The surface temperature can reach 3000 K to 5000 K (2727 °C to 4727 °C) for a gas temperature of 1000 K (727 °C).[143,144] Rajput *et al.*[13] have already reported the reduction of hematite at gas temperature as low as 573 K (300 °C).

When the stored energy in H_2* molecules exceed the dissociation energy of hydrogen molecules (4.52 eV),[73,74,109] the H_2^* molecule dissociates and forms atomic hydrogen. The H atoms incident on the reduction interface can diffuse into crystal structure.[104,106] The H atoms recombine, and the energy released by this recombination also causes heating of the surface.[65] There are several reports of surface heating by exothermic heat released during recombination at the surface.[145] The heat generation by H recombination was used in the obsolete process known as 'atomic hydrogen welding.'[63,109,145] This is a factor in the use of hydrogen in welding, cutting, and melting applications.[63,146]

Interestingly, the heat of recombination of H (4.52 eV) is more than the Fe-O bond dissociation energy (4.19 eV).[67] The heat released by H recombination is therefore sufficient to dissociate the Fe–O bond at the reduction interface.

The results of Rajput *et al.*,[13,14] who reported the reduction of iron oxide at low gas temperature in a nonthermal microwave HP, provide evidence for the importance of these heat-transfer mechanisms, since the gas temperature is insufficient to heat the iron oxide to the temperature required. Their results are considered in detail in Section VI–A.

VI. PROCESSES FOR THE REDUCTION OF IRON OXIDE BY HYDROGEN PLASMA

The benefits of HP processing of iron ore for steelmaking arise from the ability to accommodate finely divided iron ore concentrates without preagglomeration, thereby avoiding the requirement for multiple processes. Use of finely divided ores and a single step allows greater control than in the blast-furnace process. Use of a HP can potentially eliminate the need for coke ovens, agglomeration plants, blast furnaces, and oxygen steelmaking operations in future steelmaking technology.[147]

Reduction of iron ore using a HP can be carried out using both thermal and nonthermal plasmas. We consider nonthermal plasmas in Section VI–A, and thermal plasma processes in Section VI–B.

A. *Nonthermal Hydrogen Plasma Processes*

The reduction of iron oxide by nonthermal HPs take place at low temperatures, well below the melting point of iron ore. The properties of nonthermal plasmas were outlined in Section II–B, and they have been considered with reference to reaction kinetics, and energy transfer to the reaction interface, in Sections V–A and V–D, respectively.

Experimental studies of the reduction of solid-state iron oxide by nonthermal HP have been presented by Rajput *et al.*[13,14] They carried out the reduction of iron oxide at low gas temperature in a nonthermal microwave (2.45 GHz) HP. The iron oxide was in the form of compacted pellets of diameter 40 mm and thickness between 3 and 9 mm. The effects of varying process parameters including the ambient temperature and pressure, hydrogen flow rate and microwave power were investigated; results are shown in Figure 22. It was found that the HP could reduce the iron oxides even at temperatures as low as 573 K (300 °C), for which reduction by hydrogen gas is negligible. In all cases, the reduction reaction proceeded in the sequence $Fe_2O_3 \rightarrow Fe_3O_4 \rightarrow FeO$, leading to metallic Fe formation.

An approximately 95 pct reduction was achieved for all the parameters investigated. Ambient temperature had only a small influence on the reduction rate. However, the reaction rate was nearly three times faster for experiments carried out at higher microwave power and pressure. Rajput *et al.* linked the reduction rate to

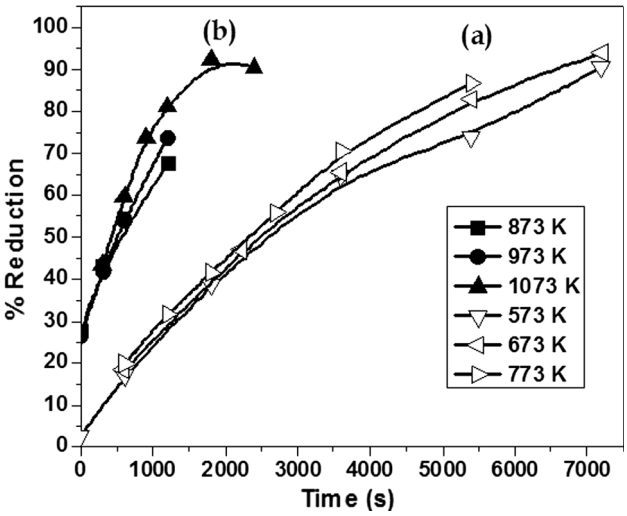

Fig. 22—Percentage reduction as a function of time at various temperatures for microwave plasma reduction of Fe_2O_3: (*a*) Set 1 [temperatures 573 K, 673 K, and, 773 K (300 °C, 400 °C, and 500 °C), power 750 W, pressure 5333 Pa]; (*b*) Set 2 [temperatures 873 K, 973 K, and 1073 K (600 °C, 700 °C, and 800 °C), power 1500 W, pressure 13 333 Pa].[13] Reproduced from Ref. [13] by permission of Taylor & Francis Ltd, http://www.tandfonline.com.

the average microwave power density (MWPD), which depended on the microwave power, hydrogen flow rate, and pressure. This determined properties of the plasma such as the electron density and temperature, gas temperature, and plasma species densities. Increasing the MWPD from 4.8 to 22.4 $\times$ 10^6 W m^{-3} increased the iron oxide reduction rate from 2.4 to 5.2 $\times$ 10^3 pct m^{-3}, where the unit is percentage reduction of the iron oxide per cubic metre of hydrogen gas. Rajput *et al*. reported a decrease in the activation energy of the iron oxide reduction reactions due to vibrationally excited hydrogen molecules; this effect has been discussed in Section V–C.

Zhang *et al*.[78] used a cold HP to reduce tablets of Fe_2O_3 to metallic iron. The plasma was a DC pulsed glow discharge at 1500 Pa, with a gap of 10 mm between the electrodes, 1250 Hz pulse frequency, 550 V voltage and 0.3 A current. Complete reduction under plasma exposure occurred after 10 mins at 763 K (490 °C), but no reduction was obtained using neutral hydrogen gas, even after 60 minutes.

The polarity was found to have a critical role, as was noted in Section III–C and shown in Figure 10. No reduction occurred when the sample was placed on the anode and only a small amount reduction occurred when the sample was electrically isolated. However, when the sample was placed on the cathode, the reduction was significant, and the overall reduction rate followed a sigmoidal-type curve, characterized by three stages of reduction with reduction rates.

These results were explained in terms of the plasma sheath that is formed adjacent to electrodes. The cathodic sheath voltage approaches the potential difference applied between the electrodes, accelerating ions toward the cathode, while the anodic sheath voltage is much lower and repels ions.

During the early stage of the reduction, when the sample is placed on the cathode, the surface of the oxide sample is electrically insulating, so the sheath voltage around the sample is low. After the first stage of reduction, a conductive metal layer is produced, so the sample surface has the same potential as the cathode. The voltage drop across the sheath is very large, and a high flux of hydrogen ions is accelerated toward the sample, increasing the rate of reduction. Subsequently, the increased thickness of the metal layer reduces transport of hydrogen to the oxide region, accounting for the reduced rate of reduction.

Diffusion of hydrogen species to the reaction interface through the product layer is thus the rate limiting step for the final stage. This indicates that the dimension of oxides particles is an important parameter in process design.

The results presented by Zhang *et al*.[78] indicate that hydrogen ions are an important species in the nonequilibrium reduction experiments. As discussed in Section III–B, reduction of iron oxide by hydrogen ions is thermodynamically more favorable than reduction by atoms and molecules. Further, the high energy of ions accelerated in the sheath may enhance chemisorption, and assist the diffusion of hydrogen species in the bulk.

There have been other efforts to reduce other oxide ores in nonequilibrium plasmas; for example Zhang *et al*.[77] studied the reduction of TiO_2 to Ti_2O_3 in a pulsed hydrogen glow discharge, and Zhang *et al*.[78] investigated the reduction of CuO to Cu in a similar plasma, finding in both cases that the plasma was much more effective than neutral hydrogen gas.

B. *Thermal Hydrogen Plasma Processes*

Thermal HP reduction is carried out above the melting point of ore. Thermal plasmas provides the thermodynamic and kinetic advantages of using hydrogen gas with external heating for reduction of fine iron ore, as does the suspension ironmaking technology described in Section VI–A. The HP combines both high temperature, which provides thermodynamic feasibility of the reduction reaction, and active hydrogen species, which give faster kinetics. This combination permits steel production in a single step without any carbon in the product.[65,148,149]

Thermal HP processes may be classified into two types: (i) liquid–HP reduction[79–92] and (ii) in-flight reduction.[8,89,150–154] Liquid–HP reduction is similar to the direct smelting process. The in-flight HP reduction is similar to fluidized-bed reactors and suspension ironmaking technology.[44]

In thermal HP processes, a thermal plasma is formed from hydrogen or an argon–hydrogen mixture. The thermal plasma may be produced using one of several methods, as discussed in Section II, for example a DC transferred arc, a DC nontransferred arc, or an inductively coupled RF discharge. The hydrogen gas molecules gain energy through collisions with the electrons, which are heated by the electric or electromagnetic field. The molecules becoming vibrationally excited, dissociate and then ionize. The dissociated and ionized species

Table III. HP Processing Route

Nonthermal HP Reduction (Low Temperature, Solid State, Below Melting Point)	Thermal HP Reduction (High Temperature, Liquid State, Above Melting Point)	
Solid–HP Reduction	Liquid–HP Reduction	In-Flight Reduction
Rajput *et al.*[13,14]	Gold *et al.*[10]	Gilles *et al.*[153]
Zhang *et al.*[77,8]	MacRae *et al.* [155]	Kitamura *et al.*[88]
	Kassabji *et al.*[157]	Saito *et al.*[154]
	Nakamura *et al.*[86]	Dayal *et al.*[8]
	Kamiya *et al.*[87]	Nikolic *et al.*[150]
	Back[79]	Tyklo *et al.*[151,152]
	Badr[80]	Choi[44]
	Nagasaka *et al.*[90]	Wang[164]
	Weigel *et al.*[89]	
	Plaul *et al.*[158]	

partially recombine at the plasma–oxide interface. This generates a large amount of heat, which supports the reduction of Fe_2O_3, an endothermic reaction.[7,78] The thermodynamic and kinetic advantages of HPs over neutral H_2 were considered in detail in Sections III and V, respectively.

The interest in HP reduction of iron ore first arose when Stokes[153] succeeded in achieving 100 pct reduction by injecting iron oxide powder along with hydrogen into a helium plasma. Chemical and physical analysis indicated that the product was 100 pct metal.

Liquid–HP reduction will be discussed in Section VI–B–1, followed by in-flight reduction in Section VI–B–2.

The literature on reduction by HP is summarized in Table III.

1. *Liquid–HP reduction*

Gold *et al.*[10] and MacRae *et al.*,[155] working at Bethlehem Steel Corporation, reported a single-stage plasma reactor, shown in Figure 23, based on the principle that the rate of the heterogeneous reduction reaction taking place at the interface between the processed material and plasma is directly proportional to the size of the interface. They enlarged the contact area by melting the fine solid particles, and increased the contact time by causing the liquid metal to flow down the cylindrical walls that formed the anode.[94] The low-temperature reducing plasma was generated in a DC arc discharge between a tungsten cathode and an annular anode. A 2:1 mixture of hydrogen and methane, serving as the reducing gas, was introduced into the cathode region.[116,155] A mixture of hydrogen and methane was chosen because it required less electrical power than either hydrogen or methane alone.

The pulverized ore concentrate (45 pct smaller than 37 μm with a closely specified grain size distribution) was injected downstream of the nozzle orifice tangentially to the strongly swirling gas plasma. The ore melted almost instantly to form a flowing film on the anode walls. The time of residence of the ore particles in anode walls was estimated to be in the range from 1 to 60 s.[94] The film serves several purposes required for reduction:

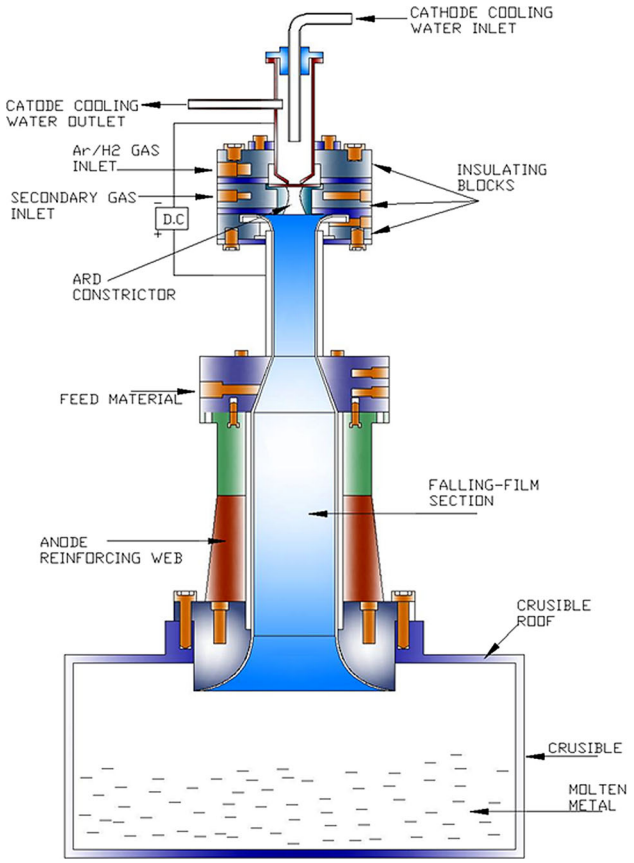

Fig. 23—Bethlehem falling-film reactor. Adapted from Ref. [10,155].

(a) It provides a large contact area between plasma gas and reactant;
(b) It provides a long residence time for heat transfer from the plasma gas;
(c) It increases the anode area, which is critical in avoiding overheating;
(d) It protects the anode from wear, particularly in the area of arc root attachment, decreasing the anode erosion rate and increasing the reactor operating lifetime;

(e) It increases the reactor efficiency by thermally insulating the walls.[116]

While the heat of the plasma is absorbed and reduction is taking place, the molten metal drops down to the magnesia crucible, which is further heated by the plasma. The slag and molten metal were collected in the magnesia crucible, which was poured intermittently.

Bethlehem Steel claimed that a H_2/CH_4 ratio of between 2:1 and 2.5:1 can reduce the electricity consumption to as little as 2.65 kWh/kg of steel with thermal efficiency 84 pct.[65,94] Other factors that were important in reducing the thermodynamic process energy requirement to close to the theoretical value (2.2 kWh/kg of iron) in scaling up the reactor from 100 kW to 1 MW were the use of finer iron ore, an improved arc heater, and improved reactor design and operation.

In spite of the promising results obtained with the Bethlehem falling-film reactor, it could not find industrial application due to difficulty in obtaining a high-power plasma torch with sufficient working life and the high working voltage needed to obtaining a stable long arc.[156] However, this 1-MW plasma pilot plant for production of iron by continuous ore reduction demonstrated that operation with economic energy requirements was feasible, and was a turning point in metallurgical application of thermal plasma for steelmaking.[147] The same unit has been employed for production of ferrochrome and ferrovanadium.[94]

A method of direct reduction of iron ore with hydrogen and natural gas plasma has also been tested at a scale of 1 MW in France. This method was found to be profitable, but only bare details were made public.[157] The 1-MW falling-film reactor pilot plant constructed under this scheme produced iron product from Carol Lake hematite with the following impurities: 50 ppm S, 10 ppm P, 60 ppm C, 60 ppm Si, and 70 ppm Cu.[147] The ore feed rate was 500 kg/hr, reducing gas feed rate was 400 m^3/h, and the molten metal was collected in the 0.6 m magnesia crucible at 320 kg/h.

Nakamura *et al.*[86] performed a laboratory-scale test, as illustrated in Figure 24, in which iron oxide was melted in a water-cooled crucible, and reduced by means of 10–50 pct H_2 mixed with Ar in a transferred-arc plasma. The degree of reduction was found to be proportional to the amount of hydrogen fed into the reactor. The efficiency of hydrogen utilization for the reduction was 50–70 pct, which is much higher than the equilibrium values below 3000 K (2727 °C). Nakamura *et al.*[86] attributed this high efficiency partly to the reactivity of the hydrogen atoms in the plasma and partly to the continuous contact of the HP with the molten iron oxide layer floating over the liquid iron that was formed. The removal of phosphorus by volatilization was remarkable. The degree of phosphorus removal depended on the $CaO/(SiO_2 + Al_2O_3)$ weight ratio. An Ar-H_2 plasma was found to give better phosphorus removal than Ar and Ar-N_2 plasmas.

Kamiya *et al.*[87] prepared a simple experimental apparatus for the study of iron ore reduction rate with both batch feeding (Figure 25) and continuous feeding (Figure 26). The apparatus comprised a DC plasma

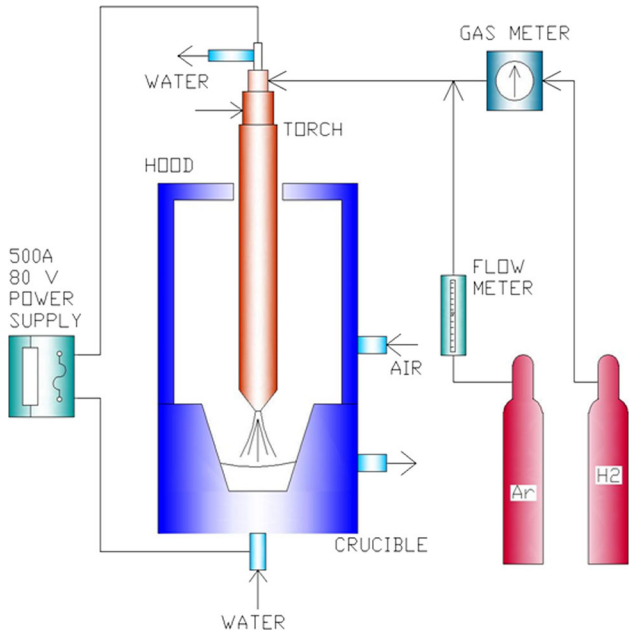

Fig. 24—Laboratory-scale transferred arc thermal plasma reactor. Adapted from Ref. [86].

torch with thoriated-tungsten electrode, water-cooled copper anode, and water-cooled copper crucible. The ore was partially melted by a nontransferred Ar plasma and then melted down by a transferred Ar plasma. The plasma gas was then switched to an Ar-H_2 (7 pct) mixture. The sample weights were between 25 to 75 g, the flow rate of the mixture gas was 20 Nl/min, and the input DC power was 8.3 kW. The reduction of molten iron oxide and FeO-bearing slags was studied. It was found that the reduction of molten iron oxides proceeded linearly with time, and the reaction rate was proportional to the atomic hydrogen partial pressure. It was thus concluded that the rate-determining step was the chemical reaction between FeO and the atomic hydrogen formed by thermal dissociation in the plasma. Further, the results showed that the rate of reduction of FeO-bearing slag was lower than that of molten iron oxide and was proportional to the FeO concentration in the slag. It was postulated that the reduction rate was also controlled by the mass transport rate of FeO across the boundary layer between the interface and the molten slag bulk. It was also observed that the reduction of both materials took place only in the cavity formed at the surface of the melt by the momentum of the plasma jet. Kamiya *et al.* also carried out continuous reduction of prereduced iron ore, as shown in Figure 26. They reported an increase in the rate of reduction for continuous feeding for all hydrogen concentrations.

Kamiya *et al.*[87] proposed a mechanism for iron oxide reduction by HP in a heterogeneous liquid–HP system that is governed by the following steps:

1. Mass transfer of hydrogen through a gas film from the bulk phase to the reaction interface between plasma gas and molten iron oxide or FeO-bearing slag;

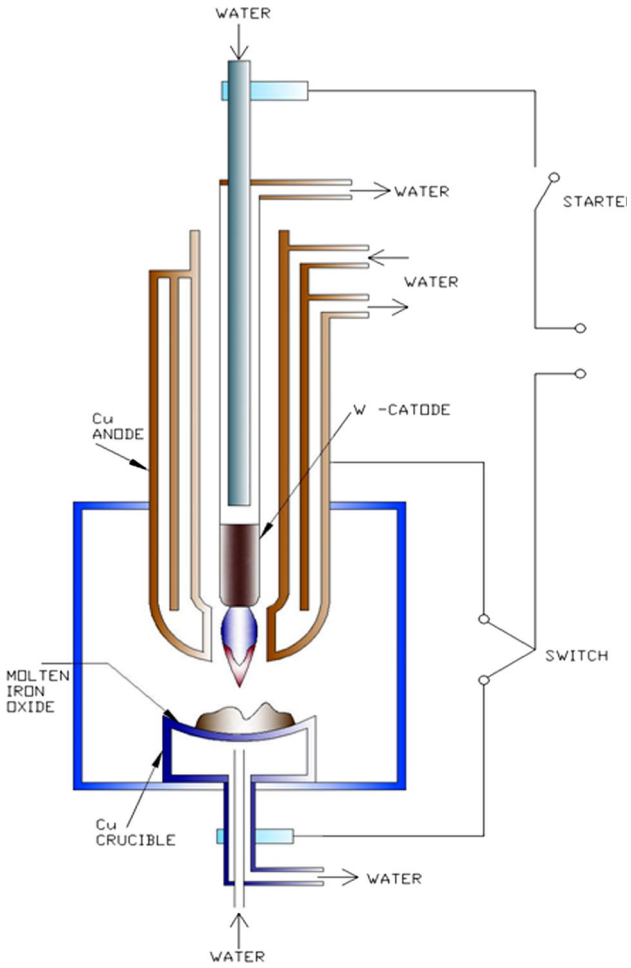

Fig. 25—Experimental reactor for batch-type feeding. Adapted from Ref. [87].

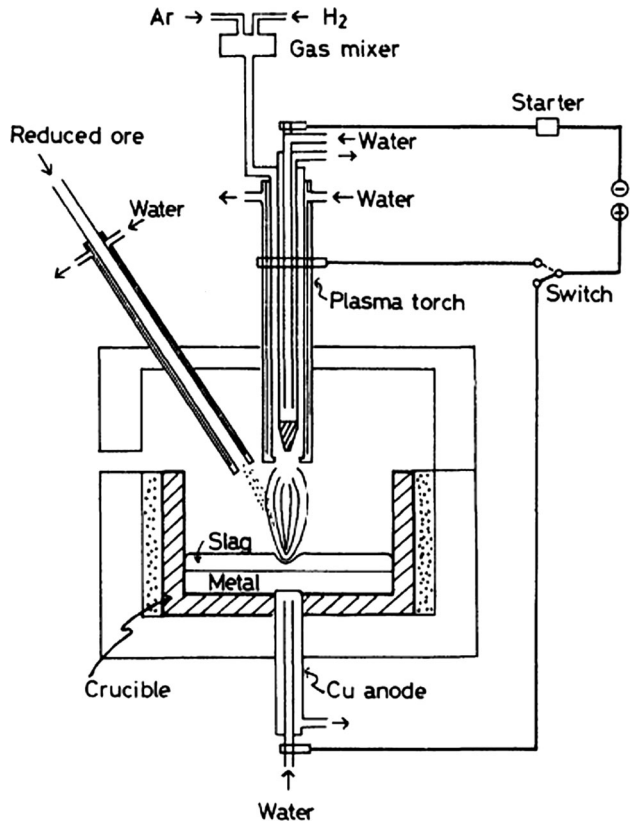

Fig. 26—Experimental reactor for continuous feeding.[87] Reproduced from Ref. [87] by permission of ISIJ International.

2. Mass transfer of oxygen through a liquid film from molten iron oxide or molten FeO-bearing slag bulk to the reaction interface;
3. Adsorption of the molecular or atomic hydrogen at the reaction interface;
4. Adsorption with dissociation of FeO at the reaction interface;
5. Chemical reaction at the reaction interface;
6. Desorption of H_2O from the reaction interface;
7. Mass transfer of H_2O through a gas film from the reaction interface to the bulk phase.

The most important work on liquid–HP reduction has been carried out as part of the European Union ULCOS programme. This is the largest initiative within the worldwide steel industry, proactively looking for solutions to the threat of global warming. As one of the candidate used in innovative steelmaking technologies, liquid–HP reduction has been examined extensively by the Chair of Metallurgy of the University of Leoben, Austria.

Hiebler and Plaul[45] demonstrated production of molten iron from its ore in a laboratory-scale experiment using HP, using a process they called Hydrogen Plasma Smelting Reduction (HPSR). Their experimental results led to the development of a concept for HPSR plant on industrial scale with the capacity to continuously produce an iron melt free of carbon and sulfur in a single stage using ore fines. A technology assessment has shown that HPSR, if it were available today, could produce steel at 20 pct lower cost than conventional steelmaking routes, with higher product quality and greater flexibility and without harming the environment.[45]

Badr[80] examined the thermodynamics, kinetics, and scale-up potential of the HPSR process in detail. A schematic overview of the plasma facility is shown in Figure 27.

Badr carried out laboratory-scale experiments using both hollow graphite and lanthanated (1 pct La_2O_3) tungsten electrodes in an 8 kW DC transferred-arc reactor, with a voltage of 110 V and current of 70 A. The fine ores were introduced in 100 g batches, or continuously fed through the hollow electrodes. The gas (H_2 or Ar-H_2) was supplied (up to a flow rate of 5 Nl/min) through the hollow electrodes, and also by lateral supply via a ceramic lance located 20 mm from the melt surface. The reduction behavior was evaluated by calculating the reduction degree, H_2 utilization degree, total H_2 utilization, and the oxygen reduction rates for 30, 40 and 50 pct Ar-H_2 mixtures.

In the earlier work of the group on liquid–HP,[79,158] it had been concluded that H and H^+ stemming from the dissociation and ionization within the plasma region took part in the reduction process at the plasma–melt

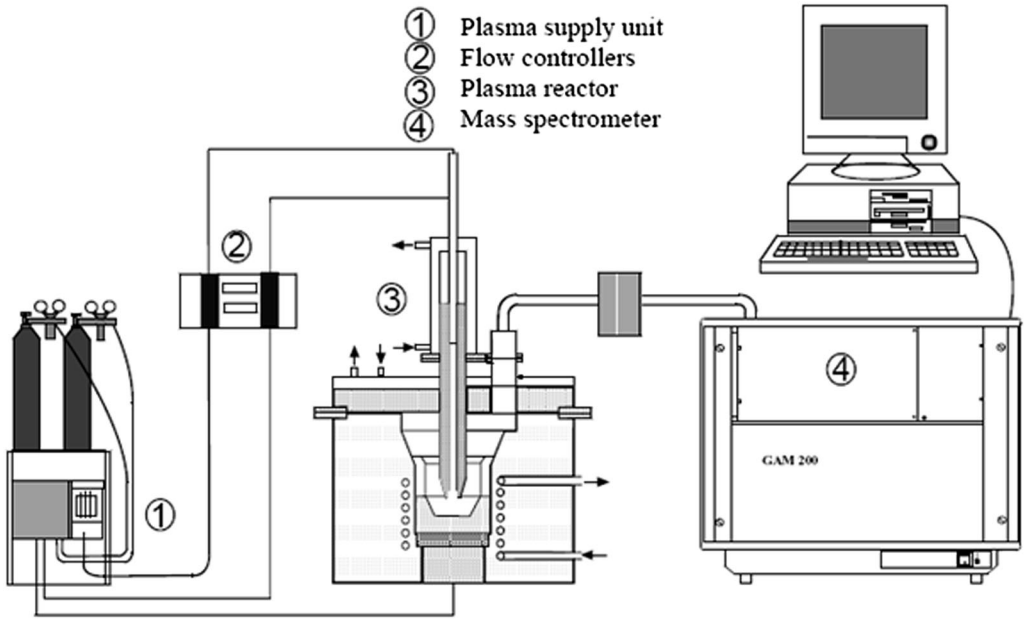

Fig. 27—Schematic overview of plasma facility.[80]

interface. This was because the reduction rates obtained in these experiments were higher than could be obtained using molecular H_2. This conclusion was re-examined by Badr,[80] by comparing results obtained with the tungsten and graphite electrodes. The results corresponded to those expected for reduction by H_2 under thermodynamic conditions, rather than by H or H^+. Badr concluded that the graphite electrodes used by Back and Plaul to ensure stability of the plasma had contributed to the increase in reduction through the formation of CO.[80] The reduction rates obtained with graphite electrodes were 1.25 times faster than with tungsten electrodes, and this was due to generation of CO; there was no evidence of reactions with HP species.[80] Badr also found that surface of the graphite electrodes was rougher than the tungsten electrodes, leading to a greater mobility of the point of arc attachment on the electrode, but stabilizing the arc contact with the melt, and ensuring that the arc did not attach to the sidewalls of the crucible. The lower surface roughness of the tungsten electrodes gave rise to a less stable arc, because the arc attached to the tip of the electrode, and the arc column moved continuously in order to find the most conducting path. This led to lateral shifting of the arc to the side walls, causing damage to the side walls.[80] Similar crucible damage was observed by Plaul.[158]

Badr *et al.*[80] investigated the reduction of hematite in the liquid state by neutral hydrogen gas and HP, and reported a decrease in activation energy due to the presence of plasma. This lowering of activation energy increased the rate of reduction of FeO by almost one order of magnitude.[87,89,90] The authors also reported that the HP reduction process was controlled by the chemical reaction rate. Hence, the interfacial area between the FeO and the HP plays a significant role in the kinetics of reduction. They also compared the reduction of FeO by HP with that by a CO plasma. They reported the activation energy for reduction by HP (23 kJ/mol) was less than one sixth of the activation energy for reduction by CO plasma (150 kJ/mol). Also, the reduction kinetics of the HP were 3.4 times faster than those of the CO plasma.

Badr[80] found that continuous feeding of the fine ores through the hollow electrode gave a stable arc and an increase in reduction rate by almost 20 pct compared with batch loading. This suggested the feasibility of continuous feeding of ore in a scaled-up process. Badr did not mention the reason for the increase in reduction rate, but it may be due to in-flight reduction, as noted earlier.

Badr[80] also examined hydrogen utilization kinetics by changing the method of hydrogen supply, testing a lateral supply of hydrogen, as shown in Figure 28, with the total hydrogen flow rate kept constant. No change in reduction was found, and the plasma–melt interfacial area remained the same.

The reduction rates of solid phase[159] and liquid phase[91,160] FeO using neutral hydrogen gas are compared with that for HPSR (liquid–HP)[79,87,161] in Figure 29.

From the figure, it is clear that the reduction potential of molecular hydrogen increases almost two orders of magnitude with respect to solid-state reduction just above the melting point. Badr[80] calculated the specific reduction rate by HP, based on the plasma–melt interfacial area, visually estimated during experimentation, and obtained a reduction rate of 0.25 kg-oxygen m^{-2} s^{-1}. Taking his transferred arc HPSR experimental data [~2673 K (2400 °C)] and the hydrogen gas smelting reduction data obtained by Hayashi *et al.*[160] at 1773 K (1500 °C) and Ban-ya *et al.*[91] at 1673 K (1400 °C), Badr obtained an activation energy of 23 kJ/mol. He observed only a small improvement in the

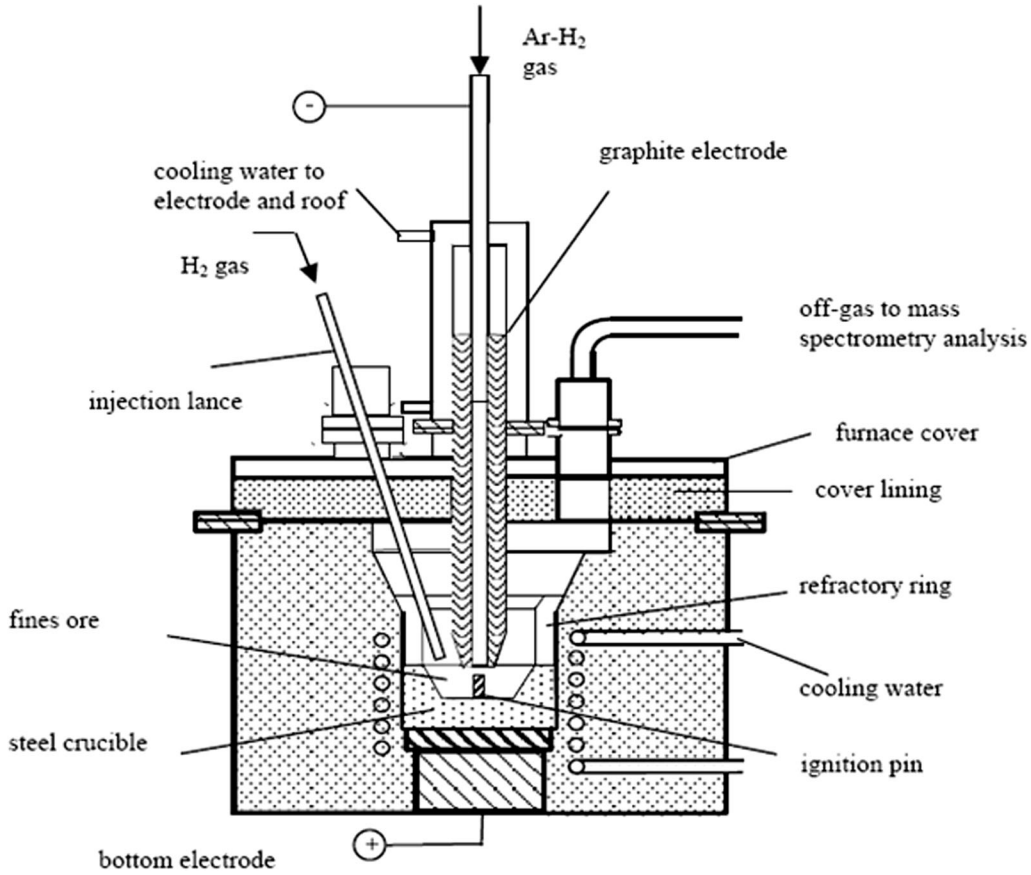

Fig. 28—Furnace layout with lateral injection of H_2.[80]

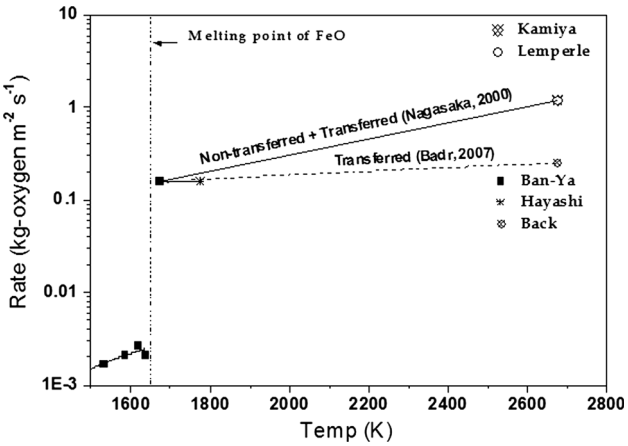

Fig. 29—Rates of reduction of FeO by neutral hydrogen[91,159,160] and hydrogen plasma[79,87,161] processes, and trends calculated by Badr[80] and Nagasaka.[90]

rate of reduction by raising the temperature up to the plasma temperature, lying within the same order of magnitude.

Nagasaka *et al.*[90] used the kinetic data of several authors[87,90,161] who used both transferred-arc and nontransferred-arc HPSR, and the hydrogen gas smelting reduction data of Hayashi *et al.*[160] at 1773 K (1500 °C) and Ban-ya *et al.*[91] at 1673 K (1400 °C), to obtain an activation energy of 80 kJ/mol. However, the rate of reduction increased almost one order of magnitude when transferred and nontransferred plasmas were combined. The authors[87,90,161] also reported that the reduction process was controlled by the chemical reaction rate. As stated earlier, Badr[80] obtained a 20 pct increase in reduction rate for continuous feeding through the hollow electrode, suggesting in-flight reduction by HP is a useful effect.

2. *In-flight reduction*

In-flight reduction has not been studied in as much detail as liquid–HP processes. Nevertheless, it has a long history; in fact the interest in HP reduction of iron ore started when Stokes[153] succeeded in achieving 100 pct reduction by injecting iron oxide powder along with hydrogen into a helium plasma. He injected the ferric oxide (Fe_2O_3) powder at a flow rate of 0.3 g/min with hydrogen as the conveying gas flowing at 13.6 L/min into a helium plasma flame operating at a power level of 15.5 kW. The product was collected by cold finger, 5 inches from the feed inlet, and was reported to be a sub-micron highly pyrophoric black powder. Chemical and physical analysis indicated that the product was 100 pct metal.

Gilles and Clumb[153] investigated the in-flight HP reduction of iron ore in a direct-current plasma jet reactor, shown in Figure 30.

The cathode (“plasma torch” in the figure) was placed on a hollow anode. The plasma gas was introduced into the space between the electrodes through the tangential slots at the outer edge of the cathode. The ore was injected through two 2.1-mm-bore orifices in the anode spaced 180° apart. The orifices were inclined at 45° to the exit plane to avoid contact between the ore particles and the anode. The plasma gas coming from the tangential slots on the outer surface of the cathode was pure hydrogen or a 3:1 mixture of argon and hydrogen. Carol Lake hematite concentrates of two sizes, −200 + 230 and −270 + 325 mesh size, were conveyed to the plasma jet by an argon stream through the orifices of anode. The oxide particles were reduced in-flight. The reduced products were collected on a water-cooled copper “quench plate”, at a distance of 146 or 197 mm downstream of the exit nozzle of the plasma jet. The reaction system was totally enclosed in a stainless steel duct that was cooled with hot water to prevent condensation of product water. The net power absorbed by the plasma gas was calculated from the difference between the total electrical energy dissipated in the electrical leads and plasma torch, and the heat removed by the cooling water. Approximately linear relationships between ore reduction and net power were obtained in all cases, as shown in Figure 31. For same net energy, pure hydrogen gave greater reduction than the 3:1 argon–hydrogen mixture. For both gas compositions, the finer-sized particles give better reduction.

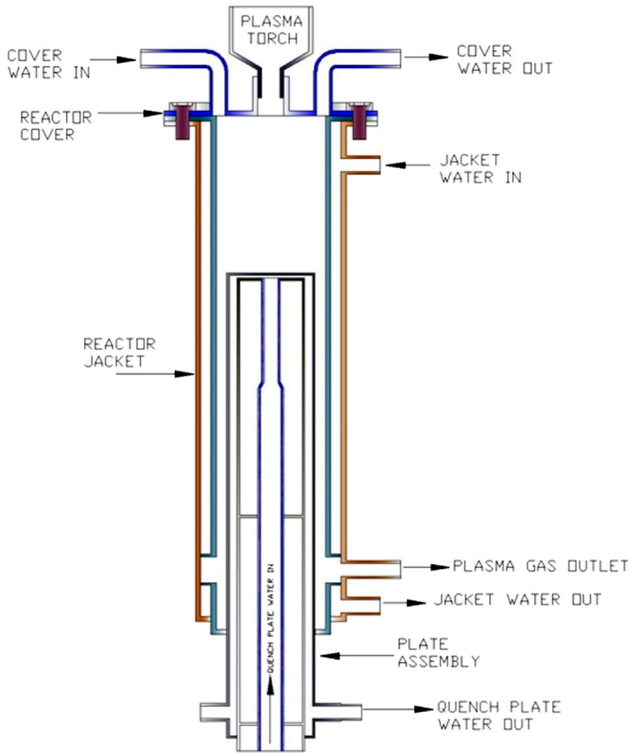

Fig. 30—Schematic of direct-current plasma reactor. Adapted from Ref. [153].

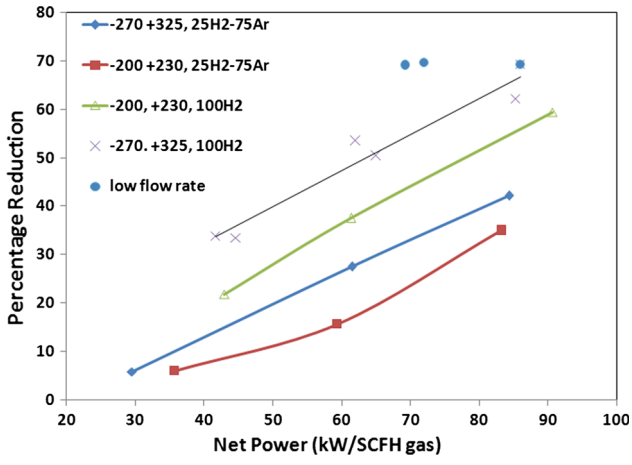

Fig. 31—Effects of plasma power on reduction, for 25 pct hydrogen in argon and 100 pct hydrogen, and different hematite particle sizes.[153]

The most important finding is that for same net power (energy per unit volume) absorbed by hydrogen gas, a lower flow rate provides better reduction. This was related to the increased residence time of particles in the hot plasma, allowing more reduction. The maximum reduction of around 70 pct was obtained using pure HP gas, finer ore size (−270 + 325) and low hydrogen flow rate.

It was concluded that the kinetics of iron oxide reduction was controlled by heat transfer to the particulates, and that the mechanism of free flight reduction varied with the rate of heat transfer. For the Ar-H_2 plasma (with lower heat-transfer rates due to the lower thermal conductivity—see Figure 13), the reduction started on the outside of the particle and layers of iron of decreasing oxidation states were formed. At the higher heat-transfer rates of the pure HP, the product iron was distributed within the particle in a continuous wustite phase, probably resulting from liquid–gas reactions.

This work further demonstrated the feasibility of iron oxide with hydrogen in a plasma reactor, but the energy requirements were approximately 100 times greater than those required theoretically. Saito *et al.*[154] performed a similar experiment and also achieved a high degree of reduction.

Kitamura *et al.*[88] carried out in-flight reduction of Fe_2O_3 in an Ar-H_2 plasma, as shown in Figure 32, to elucidate the reduction ability of thermal HP. The plasma reduced the Fe_2O_3 to metallic iron. By combining the experimental results with calculations of the equilibrium composition and of heat transfer, they explained the mechanism as follows. The oxide particles are heated quickly in the plasma, melting, and vaporizing. The vaporized oxide dissociates in the Ar–H_2 plasma to form Fe atoms. When the gas is quenched, the Fe atoms nucleate and grow to form nonspherical iron particles with the oxygen reacting with the hydrogen to form water vapor, thus avoiding oxidization of the iron during cooling. The equilibrium composition calculation is useful to predict the quenched phase and the quench temperature. The mechanism has subsequently been called “dissociative reduction”.[11]

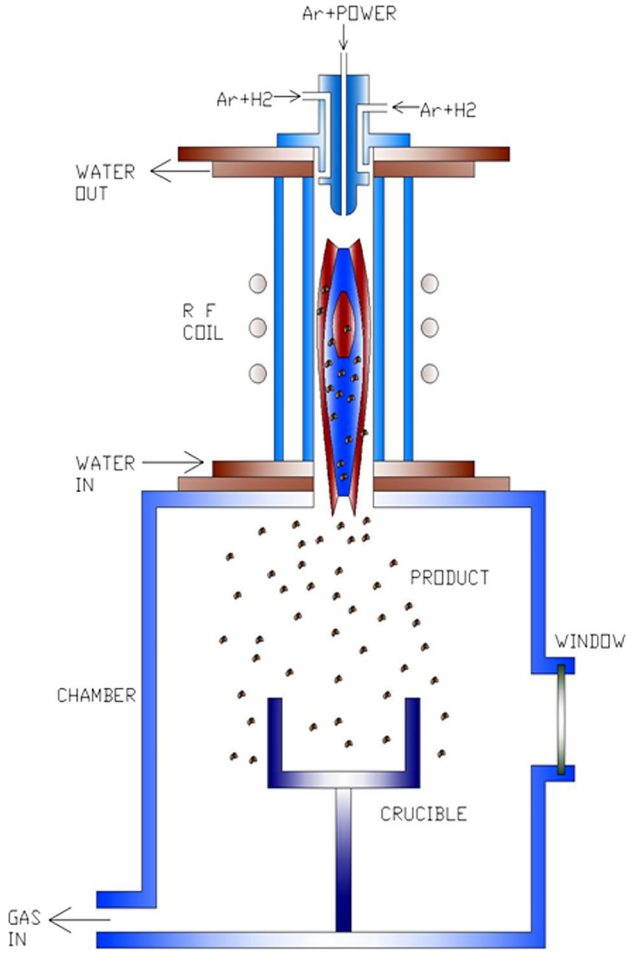

Fig. 32—Experimental setup for in-flight reduction. Adapted from Ref. [88].

Dayal *et al.*[8] designed a plasma reactor, called a ''rail reactor'', for studying the in-flight reduction of metal oxide particles. As shown in Figure 33, the reactant was introduced from the top and a transient travelling arc was produced in the rail reactor. There are three factors that were considered necessary for in-flight reduction to be successful. Firstly, high-energy atomic hydrogen should be available throughout the reaction volume to enable the reduction to proceed rapidly. Secondly, the oxide particles must be retained within the reducing atmosphere for sufficient time to be reduced. Finally, the background temperature must be well below 4400 K (4127 °C), the temperature at which water produced by the reduction would be dissociated into hydrogen and oxygen, leading to back-reactions. The rail reactor was devised to satisfy these conditions.

As shown in Figure 33, the reactor was designed such that the arc was forced to pass through the material being processed with the aim of significantly improving the plasma interaction with particles. The length of the rail electrodes, along which the arc travels, was 140 mm. It was found that the arc entrained the gas in the reactor. It was also concluded that the arc produced atomic hydrogen in a relatively large surrounding volume as it moved. The atomic hydrogen generated

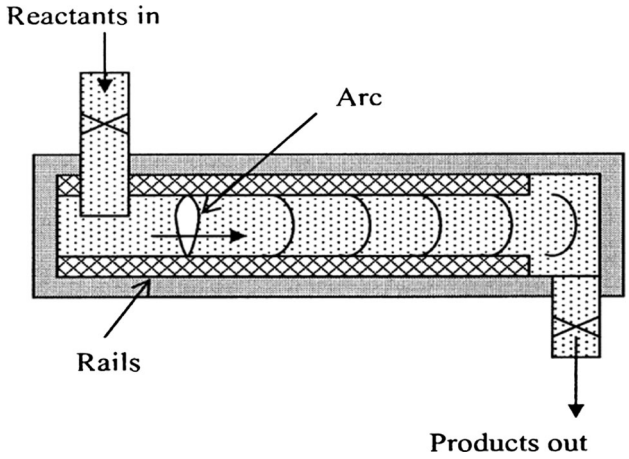

Fig. 33—Principle of rail reactor.[8] Reproduced from Ref. [8] with permission of Springer.

by the arc existed for more than 4 ms in the low-temperature background after the arc had ceased to exist, suggesting that atomic hydrogen would live for long enough to be effective in a larger practical-sized reactor. FeO in powder and tablet form was found to react more rapidly and intensely with the hydrogen treated by the arc than hot molecular hydrogen. Although more practical reactor designs are still to be explored, the results suggest that atomic hydrogen will exist throughout the volume of such a reactor for a period that is sufficient to reduce particles of FeO. Hence, it shows promise for in-flight reduction of iron oxide particles.[8] However, there were issues such as prevention of leaks, small hydrogen explosions, interruption of the arc for higher concentrations of particles, and hydrogen recombination occurring preferentially to reactions with oxygen.[162]

Sadedin *et al.*[163] also investigated an approach they termed the spark discharge method. The arrangement is shown in Figure 34. It was found that the spark discharge method at atmospheric pressure was a simple, inexpensive and relatively efficient method for producing atomic hydrogen, and hence reduction. The magnetically expanded spark was produced with 12 kV at a frequency of 1 to 200 Hz; 30 to 40 pct of spark energy was utilized, corresponding to fluxes of 3×10^{17} hydrogen atoms per discharge at a distance of 40 mm. The method was used to carry out the reduction of pellets.

Nikolic *et al.*[150] developed an 'extended arc furnace,' an arc furnace modified to produce a long stable plasma flame for in-flight reduction by introducing a hollow electrode through which gas can pass. The furnace was modified by Sadedin[162]; the 10 kW version is shown in Figure 35. In this modification, the hollow electrode is replaced by a rail reactor, through which hydrogen and argon are passed, dissociating and partially ionizing the gases. The heat of dissociation, as well as enthalpy of hot gas, is transferred to the descending cloud of FeO charge particles through the vertical chamber of the furnace. The ionized portion of the gas increases the conductivity of the arc column. The arc becomes more stable and can be extended, giving rise to more efficient

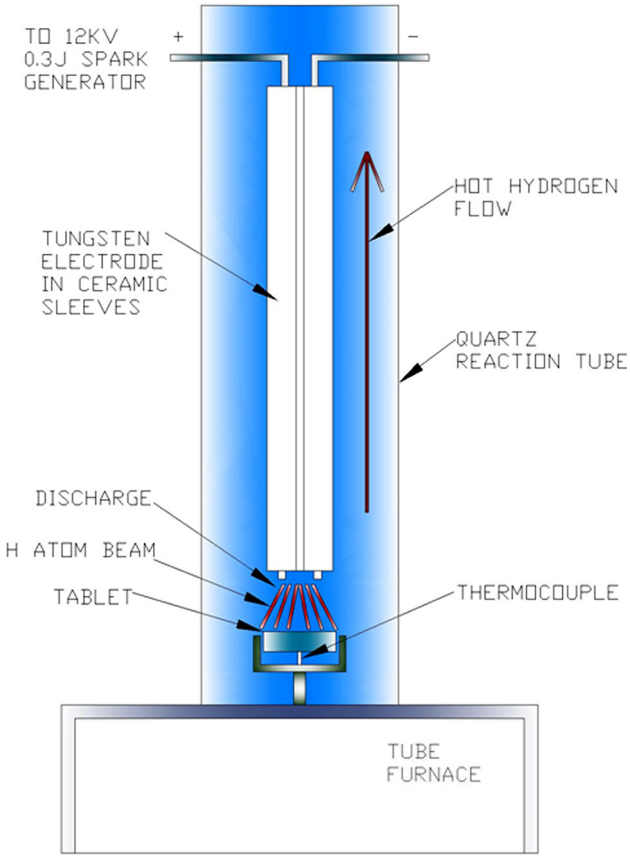

Fig. 34—Spark and magnet method. Adapted from Ref. [163].

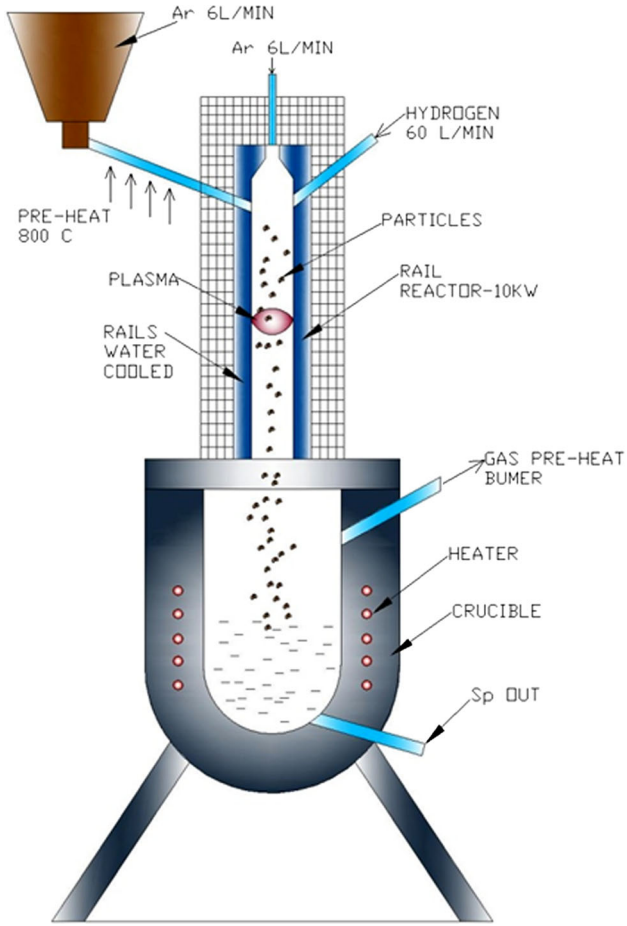

Fig. 35—Extended arc furnace. Adapted from Ref. [127], modified by Sadedin.[162]

heating. The preheated FeO is introduced from the top at nominal rates of 1 to 3 kg/h. The fall time of particles is 200 ms, in which there will be 5 passages of the 3-phase arc. The reactor design was implemented as a 30 kW furnace of 18 kg capacity for the reduction of fine ore (particle size 38 to 295 μm). The efficiency was higher than conventional plasma generators due to use of smaller particles and the fluidized bed technique.

The in-flight reduction using a "sustained shockwave plasma" is illustrated in Figure 36.[65,151,152,162] As shown in the figure, the arc is struck from the cathode and is switched from anode to anode by magnetic field coils, creating a cone of "expanded" plasma. Compression and rarefaction pressure waves are excited in the plasma by adding pulses of current to the base arc current. The pulse rate is about of 1500 Hz. Particulates of iron oxide are introduced into the reactor near the cathode, from where they fall into the cone of turbulent plasma, where ore reduction takes place.[65,151,152] Highly turbulent plasma sweeps materials into itself, causing intimate contact with the hottest and most energetic gas atoms throughout the whole volume. The objective is to "wholly entrain and process large quantities of the particulate feedstock".[162]

Recently, there have been lots of investigations of in-flight reduction by hydrogen gas. Sohn[15] carried out in-flight hydrogen-gas reduction of magnetite ore in a flash reactor (without HP) at a temperature higher than 1450 K (1177 °C) and with a particle residence time of 2 to 3 s. He obtained an activation energy of 463 kJ/mol, which indicates a relatively high temperature dependence. It was conclusively confirmed that magnetite concentrate particles can be at least 95 pct reduced by hydrogen in the several seconds of residence time typically available in a flash reactor at 1473 K (1200 °C) or above.[18]

Choi[44] reported the production of iron directly from fine magnetite ore by a gas–solid suspension technology in a high-temperature electric heating drop-tube reactor, shown Figure 37. The preheated hydrogen gas was injected into the drop-tube reactor from the top. The iron ore fines were also introduced from the top and reduced in-flight. Choi obtained 90 pct reduction at 1.6 s and almost entirely at 2.5 s at 1473 K (1200 °C) by using a large excess of hydrogen, as shown in Figure 38. His calculations demonstrated that the rate controlled by pore diffusion and mass transfer is much greater than the measured rates; *e.g.*, a 30-μm particle would be fully reduced in milliseconds under pore diffusion and mass-transfer rate control, compared with the few seconds actually observed in that study. He concluded that the reaction was not controlled by mass transfer and pore diffusion.

Following this work, Wang[164] performed comprehensive kinetics studies in the same reactor. He observed 90-99 pct reduction within 1 to 7 s at 1473 K to 1673 K

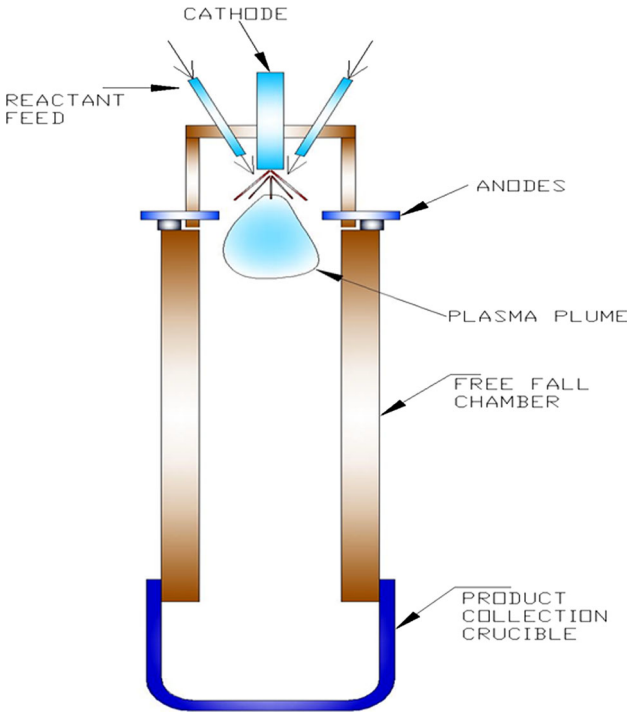

Fig. 36—The sustained shockwave plasma. Adapted from Refs. [151,152].

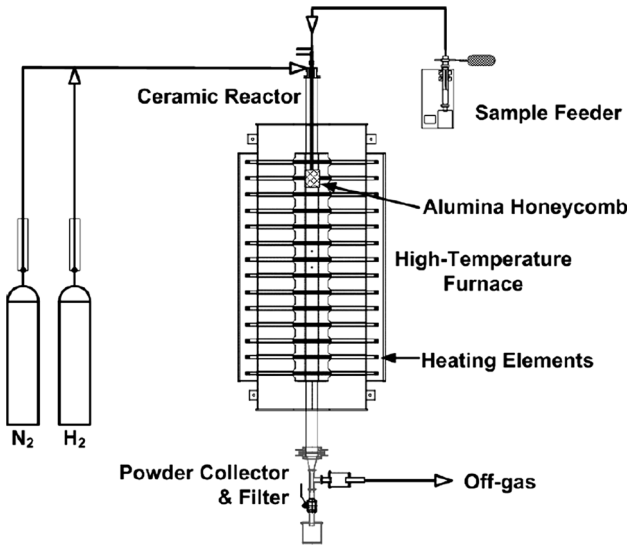

Fig. 37—Schematic diagram of a high-temperature drop-tube reactor system.[61,164] Reproduced from Ref. [61] by permission of Taylor & Francis Ltd, http://www.tandfonline.com.

(1200 °C to 1400 °C), shown in Figure 38. Wang found that rate equations describing the gas–solid reduction kinetics limited by chemical reactions at the solid surface, such as a shrinking unreacted core model, did not fit the experimental data well. After detailed calculations based on the experimental data and morphological examination, Wang showed that the nucleation and growth kinetics reported by earlier researchers[165–171] fitted the experimental results. He examined the dependence of the rate on the partial

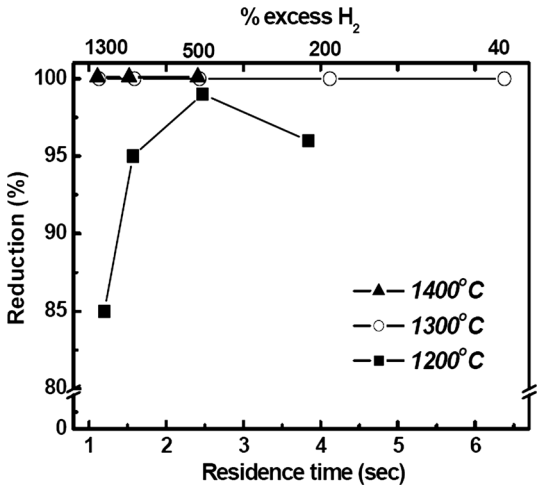

Fig. 38—Hydrogen reduction rate of iron oxide concentrate vs. residence time and percent excess H_2 at 1473 – 1673 K (1200 – 1400 °C) (particle size: 25 - 32 μm).[61] Reproduced from Ref. [61] by permission of Taylor & Francis Ltd, http://www.tandfonline.com.

pressure of hydrogen, particle size, and temperature. He found a 0.5 order dependence on the partial pressure of H_2, which is consistent with the reaction mechanism in which adsorbed H_2 molecules dissociate into H atoms before reacting with the oxide. He confirmed the chemical reaction as the rate controlling process. By applying the Arrhenius equation, he determined the activation energy to be 464 kJ/mol.

Choi[44] and Wang[164] considered the technical issue of heat supply in their studies. The use of hydrogen preheating was abandoned because the maximum possible preheating that was obtainable with commercial equipment was only about 673 K (400 °C).[44] Instead, they proposed the use of a burner or plasma torch installed on top of the reactor for heating of the charge and the hydrogen gas. Although they supported the possibility of supplying sensible heat to solid and gas feed materials with the plasma torch, they did not indicate that they had used the plasma torch in their experiments. However, their experimental results, in particular the high activation energy and residence time, indicate that the use of a HP would be attractive. In particular, use of a HP would be expected to reduce the activation energy. For example, it has been recently reported that the use of a nonthermal HP[11–14,49] in reduction lowers the activation energy, with the reduction reaction dependent on the rate of production of vibrationally excited hydrogen molecules.

VII. TECHNICAL, ECONOMIC, AND COMMERCIAL FEASIBILITY

The success of an industrial chemical plasma process requires the following stages: (a) the demonstration of technical feasibility, (b) evaluation of economic feasibility, and finally (c) commercial feasibility of a full-scale reactor. We consider these aspects in turn in this section.

A. *Technical Feasibility*

The fundamental feasibility of reduction of iron oxide by HP depends on the thermodynamics and the kinetics of the reduction reaction. HP consists of active species that increase the thermodynamic potential by lowering the Gibbs standard free energy. Further, these active species decrease the activation barrier by generating local temperature increases at the reduction interface. There is therefore ample scientific evidence that HP is capable of reducing iron oxide.

Demonstration of technical feasibility also requires experimental evidence that the process works. As shown in Section VI, this has been demonstrated in solid state[13,14,77,78] and liquid state processes.[79–92] The technical feasibility of in-flight reduction has also been reported.[8,88,150]

There are several other considerations that arise in optimizing the reduction process. For example, in solid–HP and liquid–HP cases, as the reduction starts, a metallic iron layer covering the iron oxide develops. Assuming that the diffusion of hydrogen through the metallic iron layer is not rate limiting, the extent of reduction depends on the flux of active species colliding with the iron oxide layer at the reduction interface. Since the reductant, hydrogen, is contained in the plasma working gas, the requirements for plasma production have to be balanced against the required flux of active species.

Suitable means of feeding the solid material and product collection are also required to maximize utilization of hydrogen gas. The vaporization and dissociation temperature of iron oxides are much lower than the temperatures available in a thermal HP. This indicates that care must be taken to prevent the reverse reaction if the process is carried out by thermal HP. A further requirement is that the reaction product, water, should move out of the reduction interface as the reduction reaction proceeds, in order to ensure that chemical equilibrium favors the forward reaction, *i.e.*, the formation of metallic iron.

It is clear from the above discussion that design of the plasma reactor requires balancing of several requirements, some of which are not well aligned. An optimized design must be based on experimental data coupled with theoretical considerations.

B. *Economic and Commercial Feasibility*

The primary criterion for economic feasibility of an energy-intensive process such as ironmaking is the energy consumption per unit of product, a condition needed not only to reduce operating costs but also to ensure a high throughput at lower capital cost. We consider here the estimated energy consumption in comparison to conventional processes (direct reduction and blast furnace) and the thermodynamic efficiency. A further critical consideration in the case of HP reduction of iron ore is the cost of hydrogen. Finally, for a process to be commercially feasible, it not only needs to be economic (in terms of the cost per unit product), but to be capable of a fast enough production rate to justify the construction of a plant.

1. *Energy comparison*

Sohn *et al.*[15] estimated the energy required per tonne of hot molten iron, using two methods (bond energy and heat of reaction) for the conventional blast furnace process, and for in-flight reduction (which they call "flash ironmaking") using hydrogen gas.[15] A summary is shown in Table IV.

The energy requirement for hydrogen production is strongly dependent on the production process. Therefore, the energy cost of hydrogen production was excluded from consideration from in-flight reduction; to counterbalance this, the energy required to produce coking coal was excluded for the blast furnace process.

The energy requirement for the in-flight reduction process is 65 pct or less of that for the blast furnace process. This energy saving is mainly due to the elimination of feedstock preparation such as pelletization, sintering, and cokemaking. It was assumed, to allow a fair comparison, that molten metal is produced. The energy requirement for in-flight reduction (11.51 GJ/t Fe) is somewhat more efficient than COREX (16.9 to 20.2), MIDREX (13.3), HYL III (12.3)[172,173]

2. *Thermodynamic efficiency*

Theoretically, to produce one tonne of pure iron, about 650 Nm^3 of hydrogen is required, which is equivalent to 6.5 GJ/t. This is similar to the minimum energy demand (6.8 GJ/t) when coke is used.[174] The theoretical minimum energy cost for iron production from magnetite (Fe_3O_4) and hematite (Fe_2O_3) concentrates is 7.963 GJ/t Fe. The 1 MW Bethlehem Steel reactor obtained a productivity of 318 kg/h of pure iron by using H_2/CH_4 ratio of 2:1 to 2.5:1, the energy cost was 8.640 GJ/t of steel and the thermal efficiency was 84 pct.[65]

3. *Hydrogen economy*

The cost (including the energy cost) of hydrogen is a critical factor in determining the economic viability of HP reduction. Currently hydrogen is mainly produced by reforming of methane, or by electrolysis of water. The latter approach can use electricity produced from carbon-free sources such as solar, wind, geothermal, and nuclear energy. Nuclear energy has been cited[175–181] as the optimum resource for economic production of large quantities of hydrogen.

CSM (Centro Sperimentale Metallurgico, Rome) designed direct reduction processes coupled with a nuclear reforming process. POSCO, one of the world's largest steel producers, announced plans for nuclear-based hydrogen steelmaking. Massive hydrogen production is anticipated to be obtained from small nuclear reactors. With the development of ultra-safe nuclear plants that can provide electric power for production of inexpensive hydrogen in progress, the steel industry must be ready to utilize the alternative energy. Recently, Kasahara *et al.*[182] have reported the flow diagram of a nuclear hydrogen steel plant. In this context, suspension reduction technology (similar to in-flight reduction), taking advantage of hydrogen as the reductant, is an attractive and promising alternative.[44]

Table IV. Comparison of Energy Requirements (in GJ/t Fe) for Commercial-Scale In-Flight Reduction ("Flash Ironmaking") Using Hydrogen Gas, and the Blast Furnace Process, Assuming Production of 1 Mt per Year at 1773 K (1450 °C))

Process	Blast Furnace		Hydrogen In-flight Reduction	
Approach	1	2	1	2
Reduction	7.37	2.1	6.68	0.91
Sensible heat of iron	1.35 [1873 K (1550 °C)]		1.27 [1773 K (1450 °C)]	
Sensible heat of slag	0.47 [1873 K (1550 °C)]		1.24 [1773 K (1450 °C)]	
Slurry (H_2O (l))			1.93	
Hot water not used				
Flue gas	0.26 [363 K (90 °C)]			
Removed water vapor			0.01	
$CaCO_3$ decomposition	0.33			
Slagmaking	−0.17			
Heat loss in the reactor	2.60		0.78	
Heat loss in heat exchanger(sum of next 3)	0.07		0.34	0.07
Reactor feed gas heater				
Natural gas heater				
WGS reactor feed gas heater				
Steam not used (363 K (90 °C))				
Sub-total	12.28	7.01	11.25	5.48
Pelletizing	3.01			
Sintering	0.65			
Cokemaking	2.02			
$CaCO_3$ and $MgCO_3$ calcination (external)			0.26	
Total	17.96	12.69	11.51	5.74
Percent decrease w.r.t. blast furnace	0	0	35.91	54.77

Approach 1, bond energy; Approach 2, heat of reaction.

Renewable energy, including solar and wind energy, is another attractive and nonpolluting source of the electricity necessary to produce hydrogen by electrolysis of water. Other hydrogen production processes, such as direct photocatalysis of water using semiconducting electrodes exposed to sunlight, are being actively researched.[47,48]

4. *Throughput and scale-up of the process*

A reasonable standard for throughput of a ironmaking process is that it be similar to that achieved in blast furnaces. Von Bogdandy *et al.*[53] pointed out that in order to achieve a throughput in a hydrogen reaction process equivalent to that of a blast furnace, the reduction time of iron oxide particles at 1423 K (1150 °C) should be less than 5 s.

The production of iron using the suspension process (in-flight reduction by hydrogen gas) at the University of Utah,[44,164,183] which we discussed in Section VI–B–2, meets this criterion. Choi[44] obtained 90 pct reduction at 1.6 s and almost entirely at 2.5 s at 1473 K (1150 °C) by starting with fine concentrate and using excess hydrogen. Similarly, Wang[164] obtained 93 pct reduction in a residence time of 9.3 s at 1150 °C and hydrogen pressure of 0.85 atm for a particle size 20 to 25 μm.

Choi[44] claims that the in-flight reduction process, the first flash-type ironmaking process to convert iron ore concentrates directly to metallic iron, has strong potential as a high-intensity alternative ironmaking technology, and can be adopted on a large industrial scale. Further benefits include the production of iron that does not contain carbon, and which can be therefore directly for refining without requiring a conversion step.

The R & D study at the University of Utah showed potential energy savings of 7.4 GJ/t hot metal (more than 50 pct of conventional blast furnace energy use). Based on the success of the earlier project, the American Iron and Steel Institute had initiated a subsequent Phase II-project where a larger-scale bench reactor vessel was fabricated. In 2012, University of Utah was awarded $8.9 million by the US Department of Energy to perform tests to determine the best vessel configuration and reductant to be used in a future industrial pilot

Although Choi[44] and Wang[164] succeeded in in-flight reduction by hydrogen gas, they supported using HP as a heating source. We have presented the many thermodynamic and kinetic advantages of a HP over neutral hydrogen in Sections III and V of this review. On the basis of these points, HP processing of iron ore by in-flight reduction has potential as a suitable process for commercial feasibility.

Liquid-HP reduction of iron ore also shows considerable promise as a large-scale industrial technology. However, as discussed in Section VI–B–1, before a scaled-up process can be considered, significant design work is required to maximize the flux of active species colliding with the iron oxide layer at the reduction interface, and to ensure removal of liquid iron from this region.

Scale-up of nonthermal plasma processes is more problematic. The cost of vacuum equipment means that only atmospheric-pressure systems can be considered. It

is, however, as discussed in Section V, possible to produce deviations from local thermodynamic equilibrium, such as high levels of vibrational excitation and dissociation of hydrogen molecules, even in high-intensity arc plasmas. Thus, nonthermal effects are likely to be of importance in improving the reaction rate and throughput of transferred and nontransferred arc plasma processes.

VIII. CONCLUSIONS

It has been established in this review that HP processing of iron ore is feasible both by thermal plasmas (*e.g.*, dissociative reduction using transferred arcs and in-flight reduction using nontransferred arc plasmas) and nonthermal plasmas (*e.g.*, DC glow discharge, microwave discharge). This has been done by consideration of the both the underlying physical and chemical properties of HP and its interaction with iron oxide, and detailed assessment of the existing experimental evidence.

In both thermal and nonthermal HP reduction procsses of iron ore, it has been reported that the rate of reduction of iron ore by HP is controlled by the chemical reaction rate. The reaction rate can be increased by altering thermodynamic (pressure and temperature) and kinetic (surface area, concentration, and nature of reactants) parameters.

HP offers both thermodynamic and kinetic advantages over hydrogen gas. The presence of vibrationally excited hydrogen molecules, atomic and ionic hydrogen gives thermodynamic advantages, by decreasing the Gibbs free energy of reduction. However, in a thermal plasma in local thermodynamic equilibrium (LTE), these species are present in only very low densities at the relatively low temperatures at which the heterogeneous reduction process can occur, which must be below the boiling point of iron oxide. Indeed, we have demonstrated that the densities are too low at such temperatures to make the reduction reaction thermodynamically feasible. Therefore, deviations from LTE, and vibrationally excited hydrogen molecules are of great importance. The kinetic barrier associated with HP reduction is removed by the high local temperature generated by recombination of hydrogen atoms and the de-excitation of vibrationally excited molecules at the reduction interface. The activation energy in nonthermal plasma is decreased due to vibrationally excited molecules.

The rate can also be increased by increasing the interfacial area. This can be done by using fine iron ore in an in-flight reduction process, which can be operated using a nontransferred thermal plasma. In this case, the rate of reduction is increased by almost one order of magnitude in comparison with the smelting reduction by hydrogen gas. In view of the decrease in activation energy and increase in the rate of reduction, the in-flight reduction and dissociative reduction are attractive future options for HP processing of iron ore. The thermophysical properties of the HP are critical in determining the heat transfer and the coverage area in thermal plasma processes. We have, for example, shown that adding argon to hydrogen leads to a less constricted arc, thereby increasing the interfacial area. The design of the reactor should be such that the thermophysical properties of HP are optimized for the reduction process.

Nonthermal plasmas, which are far from LTE, have been shown to be particularly effective in producing rovibrationally excited molecules. Although they have not been extensively investigated in the context of iron oxide reduction, nonthermal HPs have many properties that favor effective reduction.

We have presented an overall favorable picture for the application of HP to iron ore reduction. However, many challenges still exist. For example,

1. Development of cheap and nonpolluting methods for production of hydrogen is a prerequisite for widespread application of hydrogen and HP in steelmaking.
2. High concentrations of rovibrationally excited molecules, which are advantageous in HP reduction, are produced with lower energy cost in nonthermal plasma systems. Since only atmospheric-pressure plasma systems will be economic, design of such systems with deviations from thermal equilibrium will be important.
3. The interactions between HP with solid and liquid phases are highly complex, as are the fluid and energy flows in the reactor. For example, in a flash reactor, the reduction is dependent on the reaction temperature, the residence time of particles in the plasma zone, and the gas composition inside the reactor. These parameters depend in turn on the various physical and chemical processes occurring in the reactor, namely fluid flow, heat, and mass transfers, and the reaction of solid particles with the hot gaseous stream. Traditional chemical engineering approaches are inadequate since they do not provide information on the local gradients of temperature and HP species concentrations, which determine the interactions with the reacting particles. This makes the experimental design and scale-up of these processes highly challenging. Sophisticated three-dimensional computational fluid dynamic models are required to describe the various processes occurring in reacting gas–particle flows.
4. Development of suitable high-power plasma torches, operating on hydrogen or argon–hydrogen mixtures, is important for in-flight reduction processes. Critical issues in such torches are efficiency and electrode lifetime.
5. As in all metallurgical and chemical processes, there are many problems that have to be dealt with. In the context of HP reduction of iron ore, these include: (a) selection of the optimum HP process, (ii) method of introduction of material into the plasma zone, (iii) particle size, (iv) interface temperature, (v) residence time, (vi) avoidance of reverse reactions, in particular re-oxidation of the product, and (vii) scale-up issues.
6. Last but not the least, reduction of iron ore by HP is an interdisciplinary field that requires knowledge of

both plasma physics and metallurgical engineering. It is critical that researchers and engineers from both disciplines should work together to solve the problems and advance the technology.

REFERENCES

1. E. Basson: *World Steel in Figures*, World Steel Association, Brussels, 2015, pp. 1–30.
2. X. Zhang and E. Basson: *Sustainable Steel: at the Core of a Green Economy*, World Steel Association, Brussels, 2012, pp. 1–40.
3. R.K. Pachauri, M.R. Allen, V.R. Barros, J. Broome, W. Cramer, R. Christ, and J.A. Church: *Climate Change 2014: Synthesis Report, Contribution of Working Groups I, II and III to the Fifth Assessment Report of the Intergovernmental Panel on Climate Change*, IPCC, Geneva, Switzerland, 2014, pp. 1–151.
4. A. Carpenter: *CO_2 Abatement in the Iron and Steel Industry Report CCC/193*, IEA Clean Coal Centre, UK, 2012, pp. 1–119.
5. D.K. Matlock: *AIME Keynote and AIST J. Keith Brimacombe Memorial Lecture*, Association for Iron & Steel Technology, Warrendale, PA 15086, United States, 2014, pp. 75–89.
6. M. Johansson: PhD Dissertation No. 1586, Linkoping University, Sweden, 2014, pp. 1–97.
7. D.E. Bullard: PhD Dissertation, The University of Arizona, Tucson, AZ, USA, 1993, pp. 1–299.
8. A.R. Dayal and D.R. Sadedin: *Plasma Chem. Plasma Process.*, 2003, vol. 23 (4), pp. 627–49.
9. R.A. Palmer, T.M. Doan, P.G. Lloyd, B.L. Jarvis, and N.U. Ahmed: *Plasma Chem. Plasma Process.*, 2002, vol. 22, pp. 335–50.
10. R.G. Gold, W.R. Sandall, P.G. Cheplick, and D.R. MacRae: *Ironmak. Steelmak.*, 1977, vol. 4 (10), pp. 10–14.
11. K.C. Sabat, P. Rajput, R.K. Paramguru, B. Bhoi, and B.K. Mishra: *Plasma Chem. Plasma Process.*, 2014, vol. 34 (1), pp. 1–23.
12. K.C. Sabat, R.K. Paramguru, S. Pradhan, and B.K. Mishra: *Plasma Chem. Plasma Process.*, 2015, vol. 35 (2), pp. 387–99.
13. P. Rajput, K.C. Sabat, R.K. Paramguru, B. Bhoi, and B.K. Mishra: *Ironmak. Steelmak.*, 2014, vol. 41 (10), pp. 721–31.
14. P. Rajput, B. Bhoi, S. Sahoo, R.K. Paramguru, and B.K. Mishra: Ironmak. Steelmak., 2013, vol. 40(1), pp. 61–68(8).
15. H.Y. Sohn and M. Olivas-Martinez: *JOM*, 2014, vol. 66 (9), pp. 1557–64.
16. S. Seetharaman: *Treatise on Process Metallurgy Volume 1: Process Fundamentals*, Elsevier, Waltham, MA 02451, USA, 2014, pp. 1–952.
17. S. Seetharaman: *Treatise on Process Metallurgy Volume 2: Process Phenomena*, Elsevier, Waltham, MA 02451, USA, 2014, pp. 1–860.
18. S. Seetharaman: *Treatise on Process Metallurgy Volume 3: Industrial Processes*, Elsevier, Waltham, MA 02451, USA, 2014, pp. 1–1745.
19. H.Y. Sohn and Y. Mohassab: in *Proceedings of the World Congress on Mechanical, Chemical, and Material Engineering (MCM 2015),* Barcelona, Spain, July 20–21, 2015 pp. 336-1–336-7.
20. F. Chen, Y. Mohassab, T. Jiang, and H.Y. Sohn: *Metall. Mater. Trans. B*, 2015, vol. 46B, pp. 1133–45.
21. J. Feinman: in *The Making, Shaping and Treating of Steel,* 11th ed., D. H. Wakelin ed., The AISE Steel Foundation, Pittsburgh, PA, 1999, pp. 741–779.
22. R. Cheeley: in *Gasification Technologies Conference*, San Francisco, CA, 1999.
23. R. Quintero: *Skillings' Min. Rev.*, 1981, pp. 12–17.
24. W.O. Philbrook: *Iron Steelmak.*, 1982, pp. 12–14.
25. R. Quintero: in *Gorham/Intertech Conference on Iron & Steel Scrap, Scrap Substitutes and Direct Steel Making*, Atlanta, GA, 21–23 March 1995.
26. A. Morrison, S. Hietkamp, and D.S. van Vuuren: *Ironmak. Steelmak.*, 2004, vol. 31 (4), pp. 285–90.
27. M. Komatina and H.-W. Gudenau: *Metal. J. Metall. (MJoM)*, 2004, vol. 10 (4), pp. 309–28.
28. M. Singh and B. Björkman: *ISIJ Int.*, 2004, vol. 44 (3), pp. 482–91.
29. T. Sharma: *ISIJ Int.*, 1994, vol. 34 (12), pp. 960–63.
30. T. Sharma, R.C. Gupta, and B. Prakash: *ISIJ Int.*, 1992, vol. 32 (12), pp. 1268–75.
31. T. Sharma, R.C. Gupta, and B. Prakash: *ISIJ Int.*, 1993, vol. 33 (4), pp. 446–53.
32. S. Joo, H.G. Kim, I.O. Lee, J.L. Schenk, U.R. Gennari, and F. Hauzenberger: *Scand. J. Metall.*, 1999, vol. 28 (4), pp. 178–83.
33. A. Eberle, W. Bohrn, K. Milionis, G. Tessmer, and J. Reidetschläger: in *International Conference on Alternative Routes of Iron and Steelmaking (ICARISM)*, V. N. Misra and R. J. Holmes, eds., The Australasian Institute of Mining and Metallurgy, Victoria, Australia, 1999, pp. 201–11.
34. I.O. Lee, M.K. Shin, M. Cho, H.G. Kim, and H.G. Lee: *ISIJ Int.*, 2002, vol. 42, pp. S33–S37.
35. G. Peer: in *Industrial Fluidization South Africa* (*IFSA*), A. Luckos and P. Smit, eds., South African Institute of Mining and Metallurgy, Johannesburg, South Africa, 2005, pp. 245–55.
36. F. Hauzenberger, J. Reidetschläger, J.L. Schenk, and H. Mali: *Berg Huettenmaenn. Monatsh.* (*BHM*), 2004, vol. 149(11), pp. 385–92.
37. K. Wieder, C. Böhn, J. Wurm, and B. Vuletic: *Berg Huettenmaennische Monatshefte* (*BHM*), 2004, vol. 149(11), pp. 379–84.
38. R. Husain, S. Sneyd, and P. Weber: in *International Conference on Alternative Routes of Iron and Steelmaking* (*ICARISM*), V.N. Misra and R.J. Holmes, eds., The Australasian Institute of Mining and Metallurgy, Victoria, Australia, 1999, pp. 123–129.
39. Bresser, P. Weber, and J. Bonestell: in *68th Annual Meeting of the Minnesota Section, SME*, Center for Professional Development, University of Minnesota, Duluth, MN, 1995, pp. 17–27.
40. R.W. von Bitter, R. Husain, P. Weber, and H. Eichberger: in *International Conference on New Developments in Metallurgical Process Technology,* Dusseldorf, Germany, 1999, pp. 9–16.
41. A. Hassan, R. Whipp, K. Milionis, and S. Zeller: in *Proceedings of the Annual ISS Ironmaking Conference,* The Iron & Steel Society, Warrendale, PA*, 1994,* pp. 481–90.
42. A.D. Brent, P.L.J. Mayfield, and T.A. Honeyands: in *International Conference on Alternative Routes of Iron and Steelmaking* (*ICARISM*), V.N. Misra and R.J. Holmes, eds., The Australasian Institute of Mining and Metallurgy, Victoria, Australia, 1999, pp. 111–14.
43. T.J. Considine, C. Jablonowsk, and D.M.M. Considine: in *Final Report to National Science Foundation & Lucent Technologies Industrial Ecology Research Fellowship BES- 9727297*, US Steel Industry, USA, 2001.
44. M. E. Choi, PhD Dissertation, The University of Utah, USA., 2010.
45. H. Hiebler and J. F. Plaul: *Metallurgija*, 2004, vol. 43(3), vol. 155–62.
46. A. Zuttel, A. Borgschulte, and L. Schlapbach: *Hydrogen as a Future Energy Carrier*, Wiley, New York, 2008.
47. X.B. Chen, S.H. Shen, L.J. Guo, and S.S. Mao: *Chem. Rev.*, 2010, vol. 110 (11), pp. 6503–70.
48. A. Kudo and Y. Miseki: *Chem. Soc. Rev.*, 2009, vol. 38 (1), pp. 253–78.
49. K.C. Sabat, R.K. Paramguru, and B.K. Mishra: *Plasma Chem. Plasma Process.*, 2016, vol. 36 (4), pp. 1111–24.
50. G.H. Dieke: *J. Mol. Spectrosc.*, 1958, vol. 2 (5), pp. 494–517.
51. D. Staack, B. Farouk, A. Gutsol, and A. Fridman: *Plasma Sources Sci. Technol.*, 2008, vol. 17 (2), pp. 1–13.
52. P.J. Bruggeman, N. Sadeghi, D.C. Schram, and V. Linss: *Plasma Sources Sci. Technol.*, 2014, vol. 23 (2), pp. 1–32.
53. L.V. Bogdandy and H.J. Engell: *The Reduction of Iron Oxides*, Springer, Berlin, 1971, pp. 286–310.
54. W.M. McKewan: *Trans. Metall. Soc. AIME.*, 1960, vol. 218, pp. 2–6.
55. W.M. McKewan: *Trans. Metall. Soc. AIME.*, 1962, vol. 224, pp. 2–5.
56. E.T. Turkdogan and J.V. Vinters: *Metall. Trans. B*, 1971, vol. 2B, pp. 3175–88.
57. E.T. Turkdogan, R.G. Olsson, and J.V. Vinters: *Metall. Trans. B*, 1971, vol. 2B, pp. 3189–96.

58. K.O. Yu and P.P. Gilis: *Metall. Trans. B*, 1981, vol. 12B, pp. 111–20.
59. H.Y. Lin, Y.W. Chen, and C. Li: *Thermochim. Acta*, 2003, vol. 400, pp. 61–67.
60. A. Pineau, N. Kanari, and I. Gaballah: *Thermochim. Acta*, 2006, vol. 447, pp. 89–100.
61. M.E. Choi and H.Y. Sohn: *Ironmak. Steelmak.*, 2010, vol. 37 (2), pp. 81–88.
62. A.B. Murphy: *Plasma Chem. Plasma Process.*, 1995, vol. 15, pp. 279–307.
63. A.B. Murphy: *Plasma Chem. Plasma Process.*, 2000, vol. 20, pp. 279–97.
64. A.B. Murphy: *Chem. Phys.*, 2012, vol. 398, pp. 64–72.
65. A. Fridman: *Plasma Chemistry*, Cambridge University Press, Cambridge, 2008, pp. 1–978.
66. O. Kubaschewski and C.B. Alcock: *Metallurgical Thermochemistry*, 5th ed., Pergamon Press, Elmsford, NY, 1983, pp. 1–449.
67. M.W. Chase Jr: *NIST-JANAF Thermochemical Tables*. 4th ed., J. Phys, Chem. Ref. Data., *Monograph*, 1998, vol. 9, pp. 1–1951.
68. L. Coudurier, D.W. Hopkins, and L. Wilkomirsky: *Fundamental Metallurgical Processes, International Series on Materials Science and Technology*, Pergamon Press, Oxford, 1978, vol. 27, pp. 1–191.
69. V. Dembovsky: *Zu Fragen der Thermodynamik and reaktionkinetik in der Plasmametallurgie*, Neue Huttu, 1987, vol. 32, pp. 214–19.
70. C.V. Robino: *Metall. Mater. Trans. B*, 1996, vol. 27B, pp. 65–69.
71. M. Capitelli, I. Armenise, E. Bisceglie, D. Bruno, R. Celiberto, G. Colonna, and A. Laricchiuta: *Plasma Chem. Plasma Process.*, 2012, vol. 32 (3), pp. 427–50.
72. M. Capitelli, G. Colonna, and A. D'Angola: *Fundamental Aspects of Plasma Chemical Physics: Thermodynamics*, Springer, New York, vol. 66, 2011, pp. 1–308.
73. W.F. Giauque: *J. Am. Chem. Soc.*, 1930, vol. 52 (12), pp. 4816–31.
74. M.S. Vardya: *Mon. Not. R. Astron. Soc.*, 1965, vol. 129 (5), pp. 345–50.
75. D.M. Chizhikov, Y.V. Tsvetkov, and I.K. Tagirov: in *Mechanism and Kinetics of Reduction of Metals*, A.M. Samarin, ed., Nauka (Science), Moscow, 1970, pp. 13–26.
76. P. Lindstrom and W. Mallard: *NIST Chemistry WebBook, NIST Standard Reference Database Number 69,* National Institute of Standards and Technology, Gaithersburg MD, 20899, http://webbook.nist.gov, (retrieved October 10, 2015).
77. Y. Zhang, W.Z. Ding, S.Q. Guo, and K.D. Xu: *Trans. Nonferr. Met. Soc. China*, 2004, vol. 14 (2), pp. 317–21.
78. Y. Zhang, W. Ding, and X. Lu: *Shanghai Met.*, 2009, vol. 31 (4), pp. 15–20.
79. E. Bäck: PhD Dissertation, Montanuniversität Leoben, Austria, 1998, pp. 1–252.
80. K. Badr: PhD Dissertation, University of Leoben, Austria, 2007, pp. 1–169.
81. E. Bäck, R. Schneider, and H. Hiebler: *BHM*, 1997, vol. 142 (5), pp. 195–203.
82. E. Bäck and H. Hiebler: *BHM*, 1998, vol. 143 (5), pp. 153–58.
83. E. Bäck and A. Sormann: *BHM*, 2000, vol. 145 (1), pp. 14–21.
84. K. Badr, E. Bäck, and W. Krieger: *Symp. Proc. - Int. Symp. Plasma Chem., 18th*, Paper No. 00010, Kyoto, Japan, 2007, pp. 717.
85. K. Badr, E. Bäck, and W. Krieger: *Steel Res. Int.*, 2007, vol. 78 (4), pp. 275–80.
86. Y. Nakamura, M. Ito, and H. Ishikawa: *Plasma Chem. Plasma Process.*, 1981, vol. 1 (2), pp. 149–60.
87. K. Kamiya, N. Kitahara, I. Morinaka, K. Sakura, M. Ozawa, and M. Tanaka: *Trans. Iron Steel Inst. Jpn.*, 1984, vol. 24, pp. 7–16.
88. T. Kitamura, K. Shibata, and K. Takeda: *ISIJ Int.*, 1993, vol. 33 (11), pp. 1150–58.
89. A. Weigel, M. Lemperle, W. Lyhs, and H. Wilhelmi: *Symp. Proc. - Int. Symp. Plasma Chem., 7th*, Eindoven, Paper no. P-11-4, 1985, pp. 1214–19.
90. T. Nagasaka, M. Hino, and S. Ban-ya: *Metall. Mater. Trans.*, 2000, vol. 31B, pp. 945–95.
91. S. Ban-ya, Y. Iguchi, and T. Nagasaka: *Trans. Iron Steel Inst. Jpn.*, 1984, vol. 70, pp. 1689–96.
92. T. Soma: *Bull. Jpn. Inst. Met.*, 1982, vol. 21, pp. 620–25.
93. V. Dembovsky: *Acta. Phys. Slov.*, 1984, vol. 34 (1), pp. 11–18.
94. V. Dembovsky: *Plasma Metallurgy–The Principles*, Elsevier, New York, 1985, pp. 1–476.
95. A.B. Murphy and C.J. Arundelli: *Plasma Chem. Plasma Process.*, 1994, vol. 14 (4), pp. 451–90.
96. A. B. Murphy and E. Tam: *J. Phys. D: Appl. Phys.*, 2014, vol. 47(29), 295202.
97. J.O. Hirschfelder, C.F. Curtiss, and R.B. Bird: *Molecular Theory of Gases and Liquids*, 2nd ed., Wiley, New York, 1964.
98. M.I. Boulos, P. Fauchais, and E. Pfender: *Thermal Plasmas: Fundamentals and Applications*, 1994, vol. 1(1). Plenum Press, New York.
99. R.S. Devoto: *Phys. Fluids*, 1967, vol. 10, pp. 2105–12.
100. J. Lowke and A. B. M*urphy:* in *The Handbook of Fluid Dynamics*, R. W. Johnson, ed., CRC Pre*ss,* Boca Raton, Florida, 1998, pp. 15-1–15.32.
101. A.B. Murphy, M. Tanaka, S. Tashiro, T. Satom, and J.J. Lowke: *J. Phys. D*, 2009, vol. 42, p. 115205.
102. M. Tanaka and J.J. Lowke: *J. Phys. D*, 2007, vol. 40, pp. R1–24.
103. A.B. Murphy, M. Tanaka, S. Tashiro, K. Yamamoto, T. Sato, and J.J. Lowke: *J. Phys. D*, 2009, vol. 42, p. 194006.
104. O.G. Gabriel, W.E.N. VanHarskamp, J.J.A. VandenDungen, D.C. Schram, and R. Engeln: *Symp. Proc. - Int. Symp. Plasma Chem.*, 19th, Paper No. 115, Bochum, Germany, 2009. pp. 4.
105. K. Hassouni, A. Gicquel, M. Capitelli, and J. Loureiro: *Plasma Sources Sci. Technol.*, 1999, vol. 8 (3), pp. 494–512.
106. Y.A. Mankelevich, M.N.R. Ashfold, and J. Ma: *J. Appl. Phys.*, 2008, vol. 104, pp. 1–11.
107. S.C. Snyder, A.B. Murphy, D.L. Hofeldt, and L.D. Reynolds: *Phys. Rev. E*, 1995, vol. 52 (3), pp. 2999–3009.
108. R. Ye, A.B. Murphy, and T. Ishigaki: *Plasma Chem. Plasma Process.*, 2007, vol. 27, pp. 189–204.
109. J. Meichsner, M. Schmidt, R. Schneider, and H.E. Wagner: *Nonthermal Plasma Chemistry and Physics*, CRC Press, Boca Raton, FL, 2012.
110. P.J.W. Vankan: PhD Dissertation, TechnischeUniversiteit, Eindhoven, 2005, pp. 1-132.
111. F.F. Chen and J.P. Chang: *Lecture Notes on Principles of Plasma Processing*. Springer, New York, 2003, pp. 1–208.
112. L.F. Spencer: Doctoral Dissertation. The University of Michigan, USA (2012), pp. 1–181.
113. Y. Shimizu, Y. Kittaka, H. Matsuura, A. Nezu, and H Akatsuka: *Int. Symp. Discharges Electr. Insul. Vac.*, 23rd, Sept. 2008, vol. 2, pp. 533–36.
114. D.C. Schram, V.M. Lelevkin, and D.K. Otorbaev: *Physics of Non-Equilibrium Plasmas*, North-Holland, Amsterdam, 1992.
115. K.R. Stadler and J.B. Jeffries: *Diamond Relat. Mater.*, 1993, vol. 2, pp. 443–48.
116. R.F.G. Meulenbroeks, R.A.H. Engeln, M.N.A. Beurskens, R.M.J. Paffen, M.C.M. van de Sanden, J.A.M. van der Mullen, and D.C. Schram: *Plasma Sources Sci. Technol.*, 1995, vol. 4(1), pp. 74–85.
117. F. Hummernbrum, H. Kempkens, A. Ruzicka, H.-D. Saurent, C. Schiffert, J. Uhlenbusch, and J. Winter: *Plasma Sources Sci. Technol.*, 1992, vol. 1 (4), pp. 221–31.
118. J. Luque, W. Juchmann, and J.B Jeffries: *J. Appl. Phys.*, 1997, vol. 82(5), pp. 2072–81.
119. J. Luque, W. Juchmann, and J.B Jeffries: *J. Appl. Opt.*, 1997, vol. 36(15), pp. 3261–70.
120. V.I. Gorokhovsky: *Surf. Coat. Technol.*, 2005, vol. 194 (2), pp. 344–62.
121. L.Y. Nelson, A.W. Saunder, and A.B. Harwey: *J. Chem. Phys.*, 1971, vol. 55, p. 5127.
122. W.M. Shaub, J.W. Nibler, and A.B. Harwey: *J. Chem. Phys.*, 1977, vol. 67, p. 1883.
123. P. Capezzuto, F. Cramarossa, R. D'Agostino, and E. Molinari: *J. Phys. Chem.*, 1975, vol. 79 (15), pp. 1487–96.
124. M. Capitelli and M. Dilonardo: *Chem. Phys.*, 1977, vol. 24 (3), pp. 417–27.
125. M. Capitelli, I. Armenise, D. Bruno, M. Cacciatore, R. Celiberto, G. Colonna, O. De. Pascale, P. Diomede, F. Esposito, C. Gorse1, K. Hassouni, A. Laricchiuta, S. Longo, D. Pagano, D. Pietanza, and M. Rutiglianob: *Plasma Sources Sci. Technol.*, 2007, vol. 16, pp. S30–S44.

126. M. Capitelli,: *Int. Conf. Phenom. Ioniz. Gases, 25th*, 2001, vol. 4(1), Nagoya, Japan.
127. K. Hassouni, A. Gicquel, and M. Capitelli: *Chem. Phys. Lett.*, 1998, vol. 290 (4), pp. 502–08.
128. K. Hassouni, T.A. Grotjohn, and A. Gicquel: *J. Appl. Phys.*, 1999, vol. 86 (1), pp. 134–51.
129. P. Andre, M. Abbaoui, R. Bessege, and A. Lefort: *Plasma Chem. Plasma Process.*, 1997, vol. 17 (2), pp. 207–17.
130. P. Andre, J. Aubreton, M. Elchinger, V. Rat, P. Fauchais, A. Lefort, and A.B. Murphy: *Plasma Chem. Plasma Process.*, 2004, vol. 24 (3), pp. 435–46.
131. J. Aubreton, M. Elchinger, and P. Fauchais: *Plasma Chem. Plasma Process.*, 1998, vol. 18 (1), pp. 1–27.
132. M. Capitelli, G. Colonna, C. Gorse, P. Minelli, D. Pagano, and D. Giordano : in *AIAA 35th Thermophys. Conf.*, Anaheim, CA, 2001.
133. M Capitelli and D Giordano: *J. Thermophys. Heat Transf.*, 2002, vol. 16(2), pp. 283–85.
134. M. Capitelli, R. Celiberto, C. Gorse, C. Laricchiuta, D. Pagano, and P. Traversa: *Phys. Rev. E*, 2004, vol. 69(2), 026412.
135. K. Chen and T. Eddy: *Plasma Chem. Plasma Process.*, 1998, vol. 18 (1), pp. 29–52.
136. X. Chen and P. Han: *J. Phys. D*, 1999, vol. 32 (14), pp. 1711–18.
137. S.A. Miller and M Martinez-Sanchez: *J. Propuls. Power*, 1996, vol. 12(1), pp. 112–19.
138. V. Rat, A. Murphy, J. Aubreton, M. Elchinger, and P. Fauchais: *J. Phys. D*, 2008, vol. 41 (183), p. 001.
139. M. Van De Sanden, P. Schram, A. Peeters, J. Van Der Mullen, and G. Kroesen: *Phys. Rev. A*, 1989, vol. 40 (9), pp. 5273–76.
140. R. Sharma, G. Singh, and K. Singh: *Phys. Plasmas*, 2011, vol. 18(6), 063504.
141. A.B. Murphy: *Plasma Chem. Plasma Process.*, 2015, vol. 35, pp. 471–89.
142. A.A. Fridman and L.A. Kennedy: *Plasma Physics and Engineering*, Taylor & Francis, New York, 2004.
143. A.K. Vakar, E.G. Krasheninnikov, and E.A. Tishchenko: *Teplofizika Vysokikh Temperatur*, 1984, vol. 22, pp. 1061–66.
144. V.K. Givotov, V.D. Rusanov, and A. Fridman: *Diagnostics of Non-Equilibrium Chemically Active Plasma*, Energo-Atom-Izdat, Moscow, 1985.
145. H. Kersten, H. Deutsch, and J.F. Behnke: *Vacuum*, 1997, vol. 48, p. 123.
146. S.V. Dresvin: *Physics and Technology of Low Temperature Plasma*, Atomizdat, Moscow, 1972.
147. S.M.L. Hamblyn: *Miner. Sci. Eng.*, 1977, vol. 9 (3), pp. 151–76.
148. Y.V. Tsvetkov and S.A. Panfilov: *Low-Temperature Plasma in Reduction Processes*, Nauka (Science), Moscow, 1980.
149. N.A. Barcza, T.R. Curr, and K.U. Maske*: in Extraction Metallurgy 85*, 1985.
150. R.M. Nikolic and R.S. Segsworth: *IEEE Trans. Ind. Appl.*, 1977, vol. 13 (1), pp. 45–48.
151. J.K. Tylko: *Conf. Proc. - Int. Symp. Plasma Chem., 1st,* Kiel, Germany, 1973, pp. 2–7.
152. J.K. Tylko: *High Temperature Treatment of Material*, US Patent 8,783, 167, 1974.
153. H.L. Gilles and C.W. Clump: *Ind. Eng. Chem. Process Des. Dev.*, 1970, vol. 9 (2), pp. 194–207.
154. K. Saito, Y. Morita, K. Okabe, and K. Sanbongi: *Tetsu-To-Hagane*, 1977, vol. 63, p. 510.
155. D.R. MacRae: Method of Reducing Ore, US Patent 4002466, 1977.
156. M. Mihovsky: *J. Univ. Chem. Technol. Metall.*, 2010, vol. 45 (1), pp. 3–18.
157. F. Kassabji, *Conf. Proc. - Int. Symp. Plasma Chem.*, 4th, 1979, pp. 236–46.
158. J.F. Plaul: Doctoral Thesis, Montanuniversität Leoben, 2005.
159. S. Ban-ya, Y. Iguchi, and T. Nagasaka: *Trans. ISIJ*, 1983, vol. 23, p. 197.
160. S. Hayashi and I. Yoshiaki: *ISIJ Int.*, 1994, vol. 34 (7), pp. 555–61.
161. M. Lemperle and A. Weigel: *Steel Res.*, 1985, vol. 56 (9), pp. 465–69.
162. D.R. Sadedin: Chemical and Biomolecular Engineering, The University of Melbourne, Victoria, 3010, Personal Communication, 2013.
163. D.R. Sadedin and Z. Waven: in *Proc. XVII Int. Conf. Gas Discharges and Their Appl.* (GD 2008), Cardiff University, 7th-12th September, 2008.
164. H. Wang: Doctoral Dissertation, The University of Utah, USA, 2011.
165. Y.K. Rao: *Metall. Trans. B*, 1979, vol. 10B, pp. 243–55.
166. Y.K. Rao and M.M. Al-Kahtany: *Ironmak. Steelmak.*, 1984, vol. 11 (1), pp. 34–40.
167. Y.K. Rao and M.M. Al-Kahtany: *Ironmak. Steelmak.*, 1984, vol. 11 (2), pp. 88–94.
168. N.J. Themelis and W.H. Gauvin: *Transactions of the American Institute of Mining, Metallurgical and Petroleum Engineers*, 1963, vol. 227, pp. 290–300.
169. P.C. Hayes: *Metall. Trans. B*, 1979, vol. 10B, pp. 211–17.
170. S.K. El-Rahaiby and Y.K. Rao: *Metall. Trans. B*, 1979, vol. 10B, pp. 257–69.
171. S. Seetharaman and H. *Y.* Sohn*: in Fundamentals of Metallurgy,* S. Seetharaman, ed., Woodhead Publishing Limited, Cambridge, England, 2005, pp. 299-310.
172. L. Price, J. Sinton, E. Worrell, D. Phylipsen, H. Xiulian, and L. Ji: *Energy*, 2002, vol. 27, pp. 429–46.
173. G. Wingrove, B. Keenan, D. Satchell, and C. van Aswegen: in *Gasification Technologies Conference*, San Francisco, CA, 17–20 October 1999.
174. J.D. Beer, E. Worrell, and K. Blok: *Annu. Rev. Energy Environ.*, 1998, vol. 23, pp. 123–205.
175. L. Barreto, A. Makihira, and K. Riahi: *Int. J. Hydrogen Econ.*, 2003, vol. 28 (3), pp. 267–84.
176. J. A. Turner: *Science 305*, 2004, vol. 5686, pp. 972–74.
177. M. IAEA: in *IAEA-TECDOC-1085*, International Atomic Energy Agency, Vienna, Austria, 1999.
178. L. Walters, D. Wade, and D. Lewis: *Nuclear Energy*, 2003, vol. 42 (1), pp. 55–62.
179. J. M. Ogden: in *The Pew Center/NCEP 10-50 Workshop*, Washington, DC, 25 March 2004.
180. C.W. Forsberg: *Int. J. Hydrogen Energy*, 2007, vol. 32, pp. 431–39.
181. D. Lewis: *Prog. Nucl. Energy*, 2008, vol. 50, pp. 394–401.
182. S. Kasahara, Y. Inagaki, and M. Ogawa: *Nucl. Eng. Des.*, 2014, vol. 271, pp. 11–19.
183. H.Y. Sohn: in S. Seetharaman, A. Mclean, R. Guthriem, and S. Seetharaman, eds., *Treatise on Process Metallurgy*, vol. 3A, Elsevier, Oxford, UK and Waltham, MA 02451, USA, 2014, pp. 1596–1691.